

TI Designs

Sub-1GHzネットワーク向けエネルギー・ハーベスト周辺光/環境センサ・ノード



TI Designs リファレンス・デザイン

このTI Designは、太陽光によるエネルギー・ハーベスト技術を使用した、ワイヤレス周辺環境センシング・ソリューションのためのリファレンス・デザインです。再生可能技術を採用し、超低消費電力を特長としていることから、バックアップ電源の寿命の大幅な延長を可能にします。このリファレンス・デザインは、テキサス・インスツルメンツの超低消費電力ハーベスタ・パワー・マネージメント、SimpleLink™超低消費電力Sub-1GHzワイヤレス・マイクロコントローラ(MCU)プラットフォーム、および周囲光、湿度、温度センシング技術を使用して、エネルギー・ハーベスト回路がアクティブの間は常時監視を行い、バックアップ・バッテリーでの動作時は割り込み監視を行います。

設計リソース

TIDA-00488	デザイン・フォルダ
bq25505	プロダクト・フォルダ
CC1310	プロダクト・フォルダ
OPT3001	プロダクト・フォルダ
HDC1000	プロダクト・フォルダ
CSD75208W1015	プロダクト・フォルダ
TPD1E10B06	プロダクト・フォルダ
TIDA-00758	ツール・フォルダ

デザインの特長

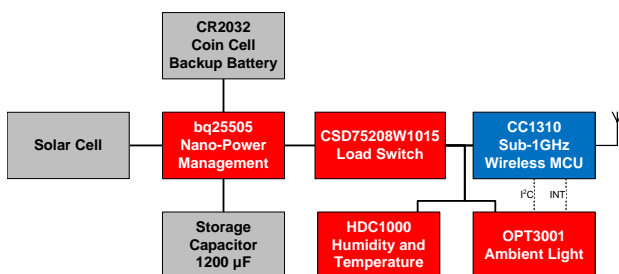
- ルクス・レベルが十分な場合はソーラー・エネルギーのみで動作(連続モード)
- ルクス・レベル条件が不十分な場合は、バックアップ・バッテリーから回路にエネルギーを供給
- ビルディングに入る自然の周囲光を検出して、ビルディングの照明システムを高精度に制御
- 周囲光に加えて温度と相対湿度も監視

主なアプリケーション

- スマート照明
- 太陽光による発電
- 環境センシング・ノード
- ワイヤレス・センサ・ノード
- モノのインターネット(IoT)
- HVACセンサ
- ビルディング・オートメーション



E2Eエキスパートに質問





使用許可、知的財産、その他免責事項は、最終ページにあるIMPORTANT NOTICE(重要な注意事項)をご参照くださいますようお願いいたします。英語版のTI製品についての情報を翻訳したこの資料は、製品の概要を確認する目的で便宜的に提供しているものです。該当する正式な英語版の最新情報は、www.ti.comで閲覧でき、その内容が常に優先されます。TIでは翻訳の正確性および妥当性につきましては一切保証いたしません。実際の設計などの前には、必ず最新版の英語版をご参照くださいますようお願いいたします。

1 Key System Specifications

表 1. Key System Specifications

PARAMETER	SPECIFICATION		DETAILS
Solar cell	IXYS IXOLAR SolarBIT (amorphous) works in indoor and outdoor locations		2.7
Non-rechargeable battery	CR2032 Lithium-ion coin cell battery (3.0-V nominal voltage)		2.6
VBAT_OV	Maximum voltage capacitor reservoir	3.50 V	4.2
VBAT_OK_HYST	Level at which capacitor reservoir is charging and becomes connected to load as the main power source	2.51 V	4.2
VBAT_OK	Level at which capacitor reservoir is discharging and becomes disconnected from load	1.90 V	4.2
Capacitor reservoir size	1200 μ F (ceramic)		4.1
Capacitor reservoir charge-up time	1000 lux	Load connect at 2.51 V from disconnect at 1.90 V	700 s
	2000 lux		250 s
	4000 lux		125 s
Power management control	When the capacitor reservoir is charging and reaches 2.5 V, the reservoir connects to the load. Once 3.5 V is reached, the reservoir disconnects from the input power source until discharged to less than 3.5 V. If the reservoir discharges to 1.9 V, the reservoir disconnects from the load.		2.4
Sensor type	Ambient light, humidity, temperature		2.1 ; 2.2
Measurement interval	Once every 15 seconds		6.1
Average off-state current consumption	1 μ A		6.3.1
On-state duration	20 ms		6.3.2
Off-state duration	14.98 s		6.3.2
Working environment	-30°C to 60°C		2.7
Form factor	2.0x3.0-in rectangular PCB		

2 System Description

Many industrial, building automation, and IoT systems require increasing numbers of wireless sensor nodes. Power distribution and consumption are two of the major constraints of adding many wireless sensor end-nodes to a system. Typical sensor end-nodes are powered by batteries, which last from several months to several years depending on the power consumption of the end node. Replacing batteries can increase the system-level cost significantly, so it is important to ensure the sensor node uses very little power to guarantee long battery life.

Additionally, many building automation systems are beginning to require ambient light sensors to monitor the effect of varying levels of natural light in the building.

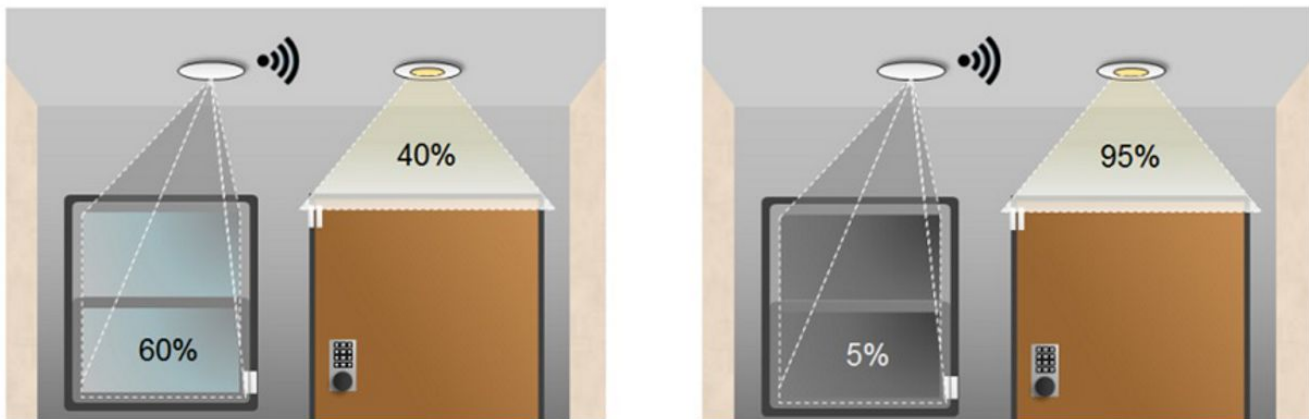


図 1. Light Sensing for Building Automation

By smartly monitoring the ambient light level, the effects of the sun coming out from behind clouds, or conversely, the natural light level decreasing due to clouds or nighttime, can be mitigated. Light control could happen through a number of methods, including automatic blind operation and artificial light level adjustments.

A major tradeoff exists between battery life and frequency of data collection for sensor nodes. If very frequent (1 to 10 seconds) data collection and transmission is required, then batteries must either have a very large capacity or be changed very frequently.

Enabled by Texas Instruments' ultra-low power harvester power management, SimpleLink ultra-low power wireless MCU platform, ambient light sensing, and humidity sensing technologies, the Energy Harvesting Ambient Light and Environment Sensor Node for Sub-1GHz Networks TI Design demonstrates an ambient light sensor node with a continual transmission mode using daylight harvesting to achieve extremely long system life with Sub-1GHz wireless communication.

This design guide addresses component selection, design theory, and the testing results of this TI Design. The scope of this design guide gives system designers a head-start in integrating TI's ultra-low power harvester power management, SimpleLink ultra-low power wireless MCU platform, ambient light sensing, and humidity sensing technologies.

2.1 Continual Transmission Mode Using Daylight Harvesting

To achieve a premium level of ambient light and environmental sensor data, it is necessary to transmit data to a central building control at a relatively high frequency (every 1 to 20 seconds). However, such high rates of sensor measurement and wireless communication results in poor system battery life. To overcome this constraint, daylight harvesting provides system power to supplement a battery for scenarios where a premium level of sensor data is required.

Daylight harvesting consists of using solar cells to power the sensor node. The solar cell collects energy from the ambient light in the installation location and feeds it to an energy harvesting power management device. The power management device buffers that solar energy into a large capacitor reservoir, and once the charge in that bank has accumulated sufficiently, the system will be powered from the reservoir. Alternatively, if sufficient charge has not been collected, a CR2032 coin cell battery provides system power. The power management device gives an indication of the actively used power source (solar cells or coin cell battery) to the wireless MCU. With this information, the wireless MCU makes measurements and wirelessly transmits less often when running from the coin cell battery to prevent its premature depletion.

2.2 Ambient Light Sensor

In this TI Design, an ambient light sensor provides an extremely accurate ambient light measurement that very closely matches the spectrum of the human eye. Knowing an accurate ambient light level enables smart buildings to accurately and intelligently control the environmental conditions to increase occupants' comfort and energy performance of the building.

The OPT3001 from Texas Instruments has flexible operating modes. This TI Design uses a low-power one-shot measurement mode and a data ready interrupt feature because the measurement rate is well-defined.

The OPT3001 is ideally suited for sensing lighting due to its ambient light linearity of 2% and rejection rate of infrared (IR) light greater than 99%. Furthermore, the OPT3001 has extremely low power consumption with an average current of 1.8 μA and an average shutdown current of 0.3 μA . Connecting the wireless MCU to this device is straightforward using an I²C interface.

2.3 Humidity and Temperature Sensor

In this TI Design, a humidity and temperature sensor was incorporated to demonstrate multiple sensing options. Similar to ambient light sensing, humidity and temperature are common measurement parameters in industrial and building automation applications.

With a relative humidity accuracy of $\pm 3\%$ and a temperature accuracy of $\pm 0.2^\circ\text{C}$, the HDC1000 can accurately sense humidity and temperature data. The HDC1000 is a very low power device, averaging 1.2 μA at a one sample per second measurement rate when active and 200 nA or less when in sleep mode. Connecting the wireless MCU to this device is straightforward using an I²C interface.

2.4 Ultra-Low Power Wireless MCU

In this TI Design, transmitting the sensor information to a central location for processing is necessary. However, because power consumption is always a concern in battery-powered applications, the radio and processor must be low power. Also, the wireless protocol required for the end-equipment system is an important consideration for the selection of the radio device.

The TI CC1310 SimpleLink ultra-low power wireless MCU platform is a low-power device with a combined radio and MCU. The CC1310 enables extremely long battery life for sensor end-nodes. Furthermore, the CC1310 is a multi-standard device with software stack support for wM-Bus and TI's SimpliciTI™ star network protocol. In this TI Design, a generic proprietary protocol was implemented, but the hardware can work with other protocols as well.

2.5 Daylight Harvester Power Management

As described previously, for applications that require a premium level of sensor data, daylight harvesting is a solution that eliminates frequent battery changes while still maintaining frequent data measurement and wireless transmission. However, to effectively use daylight energy, an intelligent energy harvester power management device is required because solar cells typically have high-output impedance and low-output voltage, which cannot directly power the rest of the sensor node devices.

In this TI Design, the bq25505 regulates the energy provided by the solar cells. The bq25505 is specifically designed to efficiently extract the microwatts (μW) to milliwatts (mW) of power generated from high-impedance solar cells without collapsing the cells. The harvested power is stored in a 1200- μF ceramic capacitor reservoir. The bq25505 also manages a CR2032 coin cell backup battery, which is used when there is not sufficient ambient light to power the sensor node.

Furthermore, the bq25505 implements several user friendly features. Users can program the voltage levels of the capacitor reservoir that allow the bq25505 to properly connect and disconnect the two power sources to the load. Users can also program the maximum power point tracking (MPPT) sampling network to optimize input power provided by the solar cell.

2.6 Low On-Resistance Load Switch

This TI Design uses a low on-resistance load switch to implement a power multiplexer that connects the wireless MCU and sensing devices to either the backup battery or capacitor reservoir. The most important characteristic of this switch is the low on-resistance. The load is always connected to either the capacitor reservoir or the backup battery through one of these load switches. Therefore, the on-resistance is a critical parameter of the load switches to prevent excess power loss that reduces the system's life.

In this design, the CSD75208W1015 was chosen as the load switch to connect the sensor nodes and MCU to the appropriate power source. Key features of this switch are the dual P-Channel MOSFETs and the 120-m Ω drain-to-drain resistance.

2.7 Coin Cell Battery

For this TI Design, a CR2032 lithium-ion coin cell battery was chosen as a back-up battery for the continual sensing operation. This battery type was chosen due to its ubiquity and small size.

The voltage characteristics for the CR2032 lithium coin cell are ideal as well. The output voltage of the battery is relatively constant until the battery is nearly depleted. At this stage, the voltage begins to decrease exponentially until the battery is depleted in full.

The temperature characteristics of lithium-ion batteries are superior to that of alkaline cells. However, the operating temperature range of the CR2032 is more limiting than the other components used in this design. Therefore, the temperature range of this TI Design is -30°C to 60°C .

Following the battery is a Schottky diode. This diode prevents damage to the other components used in this design in the case that the battery is inserted backwards. A bulk capacitor is placed in parallel with the battery to provide an energy buffer, which will prevent the battery voltage from sagging during significant current draw events. In this TI Design, the wireless MCU transmission is the source of such current draws.

2.8 Solar Cell

The IXYS IXOLAR™ High Efficiency SolarBIT solar cells (part number: KXOB22-12X1L) were chosen as the primary solar power source for this TI Design. The KXOB22-12X1L solar cell is monocrystalline and was chosen due to its small size of 0.7 × 2.2 cm per cell, 0.63-V open circuit voltage rating, and high 50.0-mA short circuit current rating.

This solar cell can operate over a wide range of electromagnetic wavelengths. Therefore, the TI Design can be used in both indoor and outdoor settings, assuming that a sufficient light level is present. The primary intended use-case for this TI Design is for indoor commercial environments.

3 Block Diagram

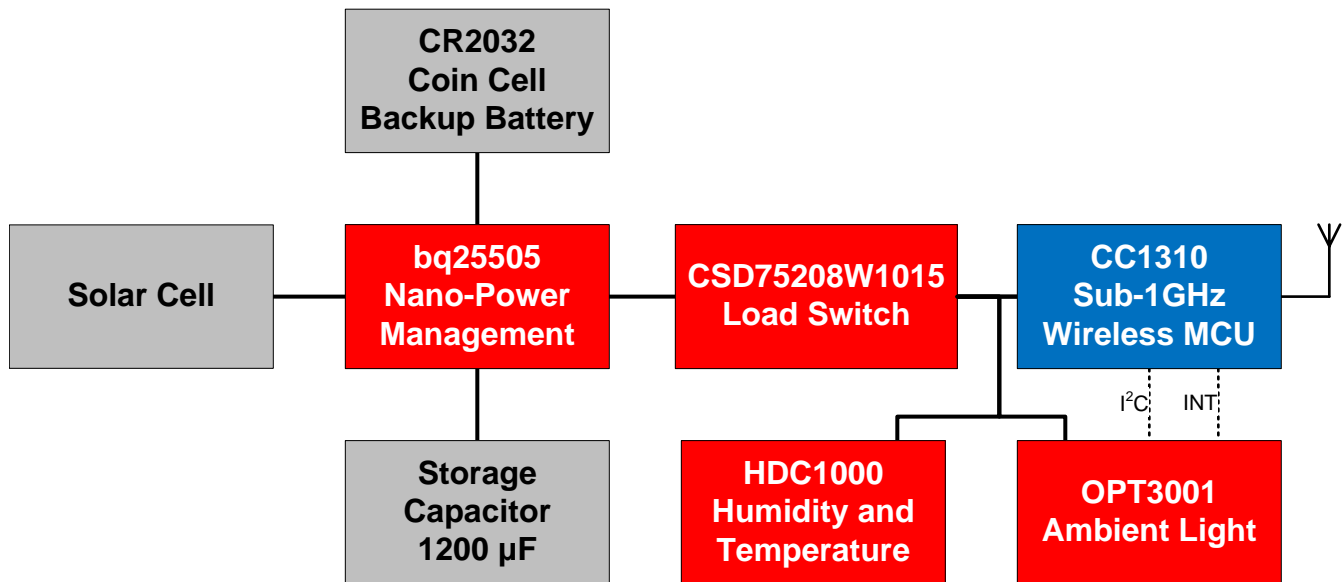


図 2. Energy Harvesting Ambient Light and Environment Sensor Node for Sub-1GHz Networks System Block Diagram

3.1 Highlighted Products

The reference design features the following devices:

- bq25505: Ultra-low power harvester power management ic with boost charger, and autonomous power multiplexor (3.1.1)
- CC1310: SimpleLink sub-1GHz ultra-low power wireless MCU (3.1.2)
- OPT3001: Digital ambient light sensor (ALS) with high precision human eye response (3.1.3)
- HDC1000: Low-power, 3% accuracy digital humidity sensor with integrated temperature sensor (3.1.4)
- CSD75208W1015: Dual common-source 20-V P-Channel NexFET™ power MOSFETs (3.1.5)
- TPD1E10B06: Single-channel ESD in 0402 package with 10-pF capacitance and 6-V breakdown (3.1.6)

For more information on each of these devices, see their respective product folders at www.ti.com.

3.1.1 bq25505

The bq25505 device is specifically designed to efficiently extract the microwatts (μW) to milliwatts (mW) of power generated from a variety of DC energy harvesting, high-impedance sources like photovoltaic (solar) or thermal electric generators (TEGs) without collapsing those sources. The battery-management features of the bq25505 ensure that a secondary rechargeable battery is not overcharged by this extracted power, with voltage boosted, nor depleted beyond safe limits by a system load. The integrated multiplexer gate drivers autonomously switch the system load to a primary nonrechargeable battery if the secondary battery voltage falls below the user-defined VBAT_OK threshold.

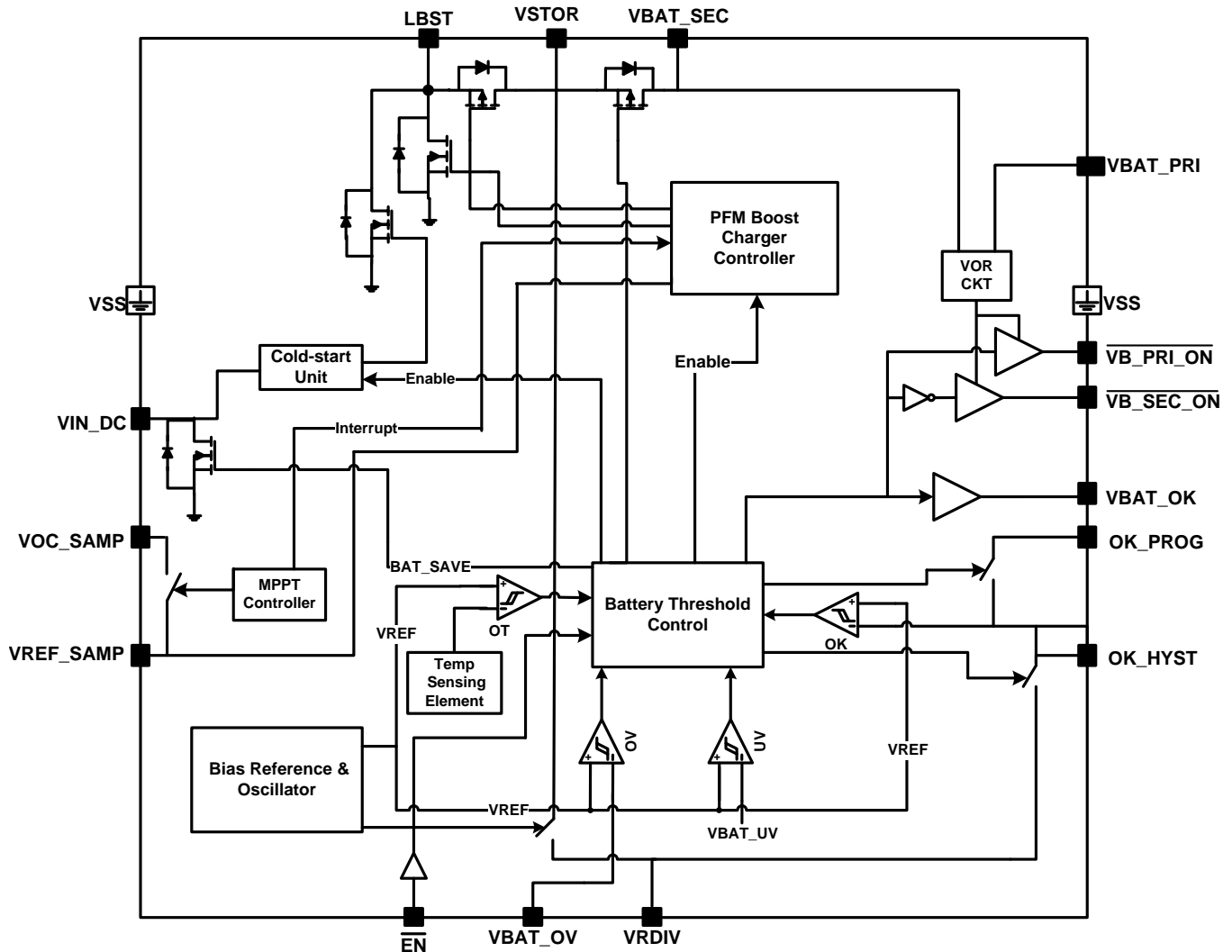


図 3. bq25505 Functional Block Diagram

Features:

- Ultra-low power with high-efficiency DC-DC boost charger
 - Cold-start voltage: $V_{IN} \geq 330$ mV
 - Continuous Energy harvesting from input sources as low as 100 mV
 - Ultra-low quiescent current of 325 nA
 - Input voltage regulation prevents collapsing high-impedance input sources
 - Ship mode with < 5 nA from battery
- Energy storage
 - Energy can be stored to rechargeable li-ion batteries, thin-film batteries, super-capacitors, or conventional capacitors
- Battery charging and protection
 - Internally set undervoltage level
 - User-programmable overvoltage level
- Battery-good output flag
 - Programmable threshold and hysteresis
 - Warn attached MCUs of pending loss of power
 - Can be used to enable or disable system loads
- Programmable MPPT
 - Integrated MPPT for optimal energy extraction from a variety of energy harvesters
- Gate drivers for primary (nonrechargeable) and secondary (rechargeable) storage element multiplexing
 - Autonomous switching based on VBAT_OK
 - Break-before-make prevents system rail droop

3.1.2 CC1310

The CC1310 is the first part in a Sub-1GHz family of cost-effective, ultra-low power wireless MCUs. The CC1310 combines a flexible, very-low power RF transceiver with a powerful 48-MHz Cortex®-M3 MCU in a platform supporting multiple physical layers and RF standards. A dedicated Cortex-M0 MCU is handling low-level RF protocol commands that are stored in ROM or RAM, thus ensuring ultra-low power and flexibility. The low-power consumption of the CC1310 does not come at the expense of RF performance; the CC1310 has excellent sensitivity and robustness (selectivity and blocking) performance. The CC1310 is a highly integrated solution offering a complete RF system solution, which includes an on-chip DC-DC converter into a true single-chip solution down to a 4x4-mm package.

Sensors can be handled in a very low power manner by a dedicated autonomous ultra-low power MCU that can be configured to handle analog and digital sensors; thus, the main MCU (Cortex-M3) sleeps for as long as possible. Software stack support for this device is as follows:

- wM-Bus
- SimpliciTI (star network)

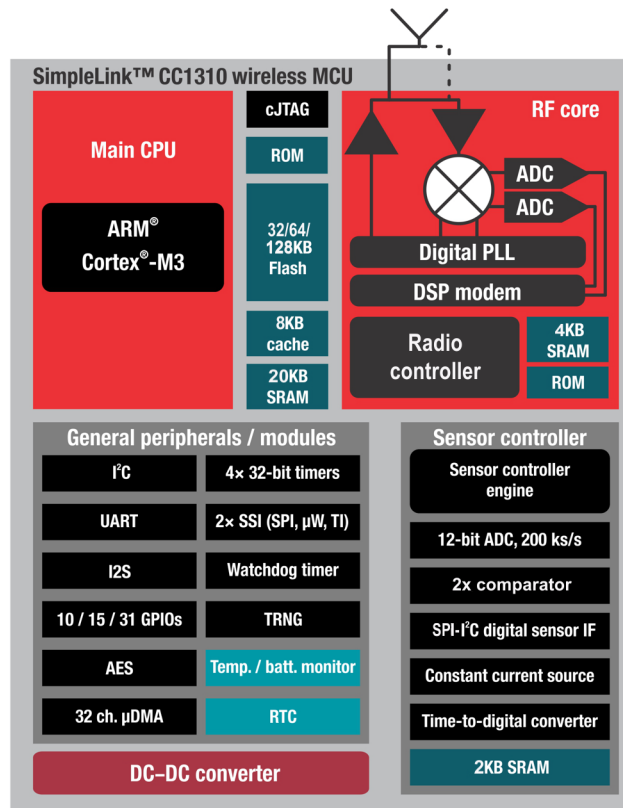


図 4. CC1310 Functional Block Diagram

Features:

- MCU:
 - Powerful ARM® Cortex-M3
 - EEMBC CoreMark score: 142
 - Up to 48-MHz clock speed
 - 128KB of in-system programmable flash

- 8KB SRAM for cache
- Up to 20-KB of ultra-low leakage SRAM
- 2-Pin cJTAG and JTAG debugging
- Supports over-the-air (OTA) upgrade
- Ultra-low power sensor controller:
 - 16-bit architecture
 - 2KB of ultra-low leakage SRAM for code and data
- Efficient code size architecture, placing peripheral drivers, RTOS, RF drivers, and bootloader in ROM
- RoHS-compliant packages:
 - 4x4-mm RSM QFN32 (10 GPIOs)
 - 5x5-mm RHB QFN32 (15 GPIOs)
 - 7x7-mm RGZ QFN48 (30 GPIOs)
- Peripherals:
 - All digital peripheral pins can be routed to any GPIO
 - 4 general-purpose timer modules (8x16-bit or 4x32-bit timer, PWM each)
 - 12-bit ADC, 200-ksps, 8-channel analog MUX
 - Continuous comparator
 - Ultra-low power analog comparator
 - Programmable current source
 - UART
 - 2 x SSI (SPI, μ W, TI)
 - I²C
 - I²S
 - Real-time clock (RTC)
 - AES-128 security module
 - True random number generator (TRNG)
 - Support for eight capacitive sensing buttons
 - Integrated temperature sensor
- External system:
 - World's smallest sub-1 GHz wireless MCU: 4 x 4 mm
 - On-chip internal DC-DC converter
 - Very few external components
 - Seamless integration with the SimpleLink CC1190 range extender
 - Pin compatible with the SimpleLink CC26xx
- Low power:
 - Wide supply voltage range:
 - Normal operation: 1.8 to 3.8 V
 - External regulator mode: 1.65 to 1.95 V

- Active-mode RX: 5.5 mA
- Active-mode TX at 10 dBm: 12 mA; 14 dBm: 25 mA
- Active-mode MCU: 61 μ A/MHz
- Active-mode MCU: 48.5 CoreMark/mA
- Active-mode sensor controller: 8.2 μ A/MHz
- Standby: 0.7 μ A (RTC running and RAM/CPU retention)
- Shutdown: 100 nA (wakeup on external events)

- RF section:
 - Excellent receiver sensitivity:
 - –121 dBm at 2.4 kbps
 - –111 dBm at 50 kbps
 - Very good selectivity and blocking performance
 - Data rate up to 4 Mbps
 - Modulation support: MSK, FSK, GFSK, OOK, ASK, 4GFSK, CPM (shaped-8 FSK)
 - Highly flexible RF modem (software-defined radio) to also cover legacy and proprietary communication protocols
 - Programmable output power up to 15 dBm with shared RX and TX RF pins (regulated power supply)
 - Antenna diversity
 - Coding gain
 - Suitable for systems targeting compliance with worldwide radio frequency regulations:
 - ETSI EN 300 220, EN 303 131, EN 303 204 (Europe)
 - FCC CFR47 Part 15 (US)
 - ARIB STD-T108 (Japan)
- Tools and development environment:
 - Full-feature and low-cost development kits
 - Multiple reference designs for different RF configurations
 - Packet sniffer PC software
 - Sensor controller studio
 - SmartRF™ Studio
 - SmartRF Flash Programmer 2
 - IAR Embedded Workbench® for ARM
 - Code Composer Studio™

3.1.3 OPT3001

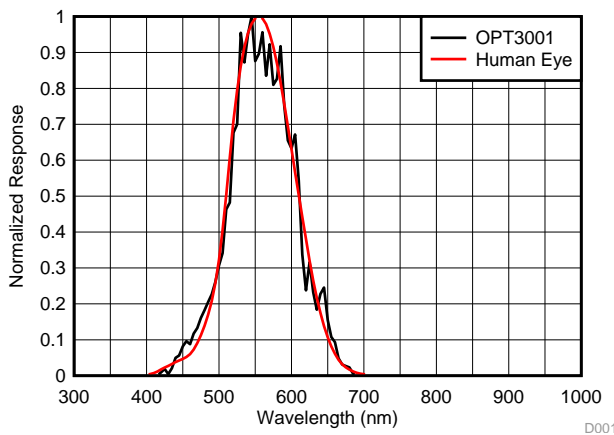
The OPT3001 is a sensor that measures the intensity of visible light. The spectral response of the sensor tightly matches the photopic response of the human eye and includes significant infrared rejection.

The OPT3001 is a single-chip lux meter, measuring the intensity of light as visible by the human eye. The precision spectral response and strong IR rejection of the device enables the OPT3001 to accurately meter the intensity of light as seen by the human eye regardless of light source. The strong IR rejection also aids in maintaining high accuracy when industrial design calls for mounting the sensor under dark glass for aesthetics. The OPT3001 is designed for systems that create light-based experiences for humans, and an ideal preferred replacement for photodiodes, photoresistors, or other ambient light sensors with less human eye matching and IR rejection.

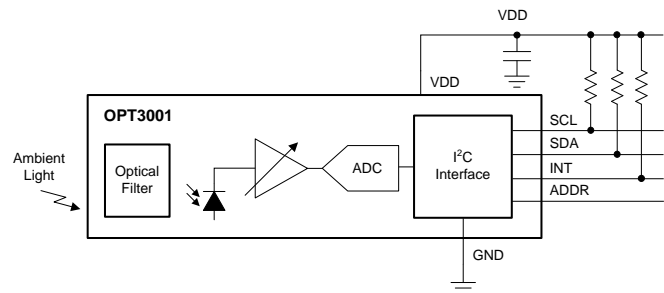
Measurements can be made from 0.01 lux up to 83k lux without manually selecting full-scale ranges by using the built-in, full-scale setting feature. This capability allows light measurement over a 23-bit effective dynamic range.

The digital operation is flexible for system integration. Measurements can be either continuous or single-shot. The control and interrupt system features autonomous operation, allowing the processor to sleep while the sensor searches for appropriate wake-up events to report through the interrupt pin. The digital output is reported over an I²C- and SMBus-compatible, two-wire serial interface.

The low power consumption and low power supply voltage capability of the OPT3001 enhance the battery life of battery-powered systems.



5. Spectral Response of OPT3001 and Human Eye



6. OPT3001 Functional Block Diagram

Features:

- Precision optical filtering to match human eye:
 - Rejects > 99% (typ) of IR
- Automatic full-scale setting feature simplifies software and ensures proper configuration
- Measurements: 0.01 lux to 83k lux
- 23-bit effective dynamic range with automatic gain ranging
- 12 binary-weighted full-scale range settings: < 0.2% (typ) matching between ranges
- Low operating current: 1.8 μ A (typ)
- Operating temperature range: -40°C to 85°C

- Wide power-supply range: 1.6 to 3.6 V
- 5.5-V tolerant I/O
- Flexible interrupt system
- Small-form factor: 2.0 × 2.0 × 0.65 mm

3.1.4 HDC1000

The HDC1000 is a digital humidity sensor with integrated temperature sensor that provides excellent measurement accuracy at very low power. The device measures humidity based on a novel capacitive sensor. The humidity and temperature sensors are factory calibrated. The innovative Wafer Level Chip Scale Package (WLCSP) simplifies board design with the use of an ultra-compact package. The sensing element of the HDC1000 is placed on the bottom part of the device, which makes the HDC1000 more robust against dirt, dust, and other environmental contaminants. The HDC1000 is functional within the full -40°C to 125°C temperature range.

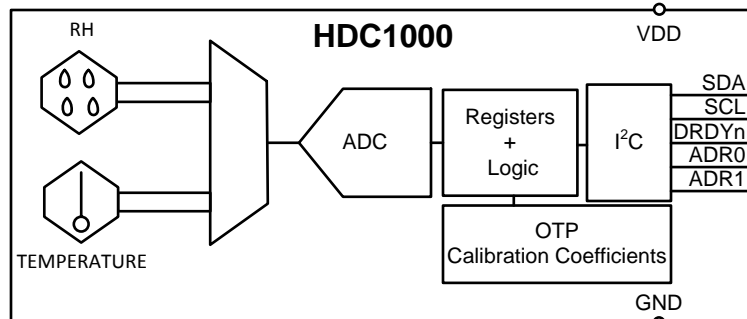


図 7. HDC1000 Functional Block Diagram

Features:

- Relative humidity (RH) operating range: 0% to 100%
- 14-bit measurement resolution
- Relative humidity accuracy: $\pm 3\%$
- Temperature accuracy: $\pm 0.2^{\circ}\text{C}$
- 200-nA sleep mode current
- Average supply current:
 - 820 nA at 1sps, 11-bit RH measurement
 - 1.2 μA at 1sps, 11-bit RH and temperature measurement
- Supply voltage: 3 to 5 V
- Tiny 2x1.6-mm device footprint
- I²C interface

3.1.5 CSD75208W1015

This device is designed to deliver the lowest on-resistance and gate charge in the smallest outline possible with excellent thermal characteristics in an ultra-low profile. Low on-resistance coupled with the small footprint and low profile make the device ideal for battery operated space constrained applications.

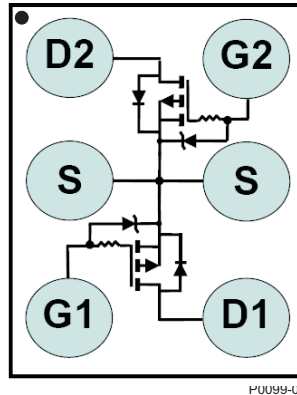


図 8. CSD75208W1015 Device Configuration

Features:

- Dual P-channel MOSFETs
- Common source configuration
- Small footprint: 1 × 1.5 mm
- Gate-source voltage clamp
- Gate ESD protection: -3 kV
- Pb free
- RoHS compliant
- Halogen free

3.1.6 TPD1E10B06

The TPD1E10B06 device is a single-channel electrostatic discharge (ESD) transient voltage suppression (TVS) diode in a small 0402 package. This TVS protection product offers ± 30 -kV contact ESD, ± 30 -kV IEC air-gap protection, and has an ESD clamp circuit with a back-to-back TVS diode for bipolar or bidirectional signal support. The 12-pF line capacitance of this ESD protection diode is suitable for a wide range of applications supporting data rates up to 400 Mbps. The 0402 package is an industry standard and is convenient for component placement in space-saving applications.

Typical applications of this ESD protection product are circuit protection for audio lines (microphone, earphone, and speaker phone), SD interfacing, keypad or other buttons, VBUS pin and ID pin of USB ports, and general-purpose I/O ports. This ESD clamp is good for the protection of the end equipment like ebooks, tablets, remote controllers, wearables, set-top boxes, and electronic point of sale equipment.

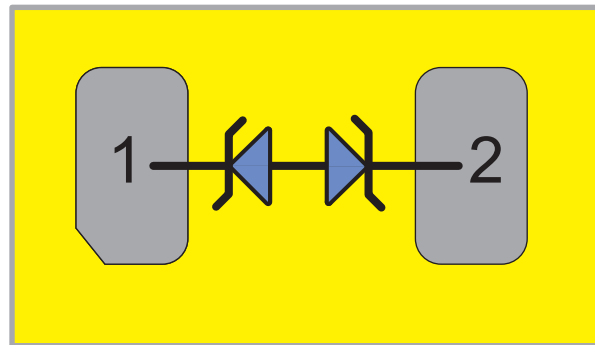


図 9. TPD1E10B06 Functional Block Diagram

Features:

- Provides system-level ESD protection for low-voltage IO interface
- IEC 61000-4-2 level 4
- ± 30 -kV (air-gap discharge)
- ± 30 -kV (contact discharge)
- IEC 61000-4-5 (surge): 6 A (8/20 μ s)
- IO capacitance: 12 pF (typical)
- RDYN: 0.4 Ω (typical)
- DC breakdown voltage: ± 6 V (minimum)
- Ultra-low leakage current: 100 nA (maximum)
- 10-V clamping voltage (maximum at IPP = 1 A)
- Industrial temperature range: -40°C to 125°C
- Space-saving 0402 footprint (1.0 \times 0.6 \times 0.5 mm)

4 System Design Theory

The Energy Harvesting Ambient Light and Environment Sensor Node for Sub-1GHz Networks TI Design measures ambient light, relative humidity, and temperature, while achieving an extremely long battery life. The following sections describe in more detail the theory used to properly design this sensor node.

4.1 Continual Transmission Mode Using Daylight Harvesting Design Theory

For applications that require a premium level of sensor data, meaning that wireless transmissions of data occur every few seconds, the continual transmission mode of this TI Design is required. In this instance, as described previously, it is necessary to provide power using solar cells and the bq25505. Otherwise, batteries would have to be constantly changed.

The following subsections describe the design aspects necessary to ensure proper operation of the continual transmission mode.

4.1.1 Capacitor Reservoir Selection

The main parameters that affect the amount of energy needed to continuously collect and transmit environment data are:

- Current consumed by sensor nodes and MCU (mA)
- Desired maximum change in voltage of capacitor reservoir during energy required event (V)
- Amount of time during an energy required event (ms)

式 1 describes the amount of capacitance needed to supply energy to the MCU and the sensor nodes for this TI Design:

$$C > \frac{I_{ON} \times \Delta T_{ON}}{\Delta V_{CAP}} \quad (1)$$

When choosing the maximum change in voltage, consider the desired setting of the overvoltage threshold on the bq25505 and the programmed VBAT_OK setting. This change in voltage should be less than the difference between these two values.

When performing this calculation, focus on the values of the highest energy occurring events. For this TI Design, the initial powering of the CC1310 and sensor nodes and the transmission of a signal by the CC1310 were examined. During each of these events, a large amount of current is drawn.

4.1.2 Capacitor Reservoir Operating Range

For the continual transmission mode, the power management of the bq25505 must be configured appropriately. This includes setting an appropriate voltage range condition where the load is receiving energy from the capacitor reservoir (VBAT_SEC) instead of from the backup battery (VBAT_PRI). VBAT_OK_PROG indicates when the capacitor reservoir has discharged to an unacceptable amount. When this occurs, the load will start receiving energy from the backup battery and enable the capacitor reservoir to recharge. VBAT_OK_PROG can be set with an external voltage divider based on 式 2:

$$VBAT_OK_PROG = VBIAS \left(1 + \frac{R_{OK2}}{R_{OK1}} \right) \quad (2)$$

When the capacitor reservoir is charging, the threshold to switch the energy supplied to the sensor nodes and MCU from the battery to the capacitor reservoir can be set with an external voltage divider based on 式 3:

$$VBAT_OK_HYST = VBIAS \left(1 + \frac{R_{OK2} + R_{OK3}}{R_{OK1}} \right) \quad (3)$$

The sum of the resistors is recommended to be no higher than approximately:

$$R_{OK1} + R_{OK2} + R_{OK3} = 13 \text{ M}\Omega \quad (4)$$

The logic high level of this signal is equal to the VSTOR voltage and the logic low level is ground. The logic high level has ~20 k Ω internally in series to limit the available current to prevent MCU damage until it is fully powered. The VBAT_OK_PROG threshold must be greater than or equal to the UV threshold.

If the capacitor reservoir is supplying energy to the load while it is charging and reaches its overvoltage value, the bq25505's internal power management stops charging the capacitor reservoir, allowing it to slightly discharge and preventing it from damaging the sensor nodes and MCU. This overvoltage threshold can be set by an external resistor divider based on 式 5:

$$VBAT_OV = \frac{3}{2} VBIAS \left(1 + \frac{R_{OV2}}{R_{OV1}} \right) \quad (5)$$

The sum of the resistors is recommended to be no higher than 13 M Ω (that is, ROV1 + ROV2 = 13 M Ω).

4.1.3 Maximum Output Power Point Tracking (MPPT)

High impedance DC sources have a maximum output power point (MPP) that varies with ambient conditions. For this TI Design, MPPT must be used to receive the maximum amount of input power from the solar panel. A solar panel's MPP varies with the amount of light shined on the panel as well as the temperature. The datasheet of the selected solar panel should list the typical MPP open circuit voltage and short circuit current, both of which are a percentage of their original amount. An external voltage divider can be set by 式 6:

$$\frac{R_{OC2} + 10 \text{ M}\Omega}{R_{OC1} + R_{OC2} + 10 \text{ M}\Omega} = \frac{V_{OC_MPP}}{V_{OC}} \quad (6)$$

4.2 Firmware Control

The firmware for the TIDA-00488 is designed for continual transmission, where data packets will be transmitted at set intervals.

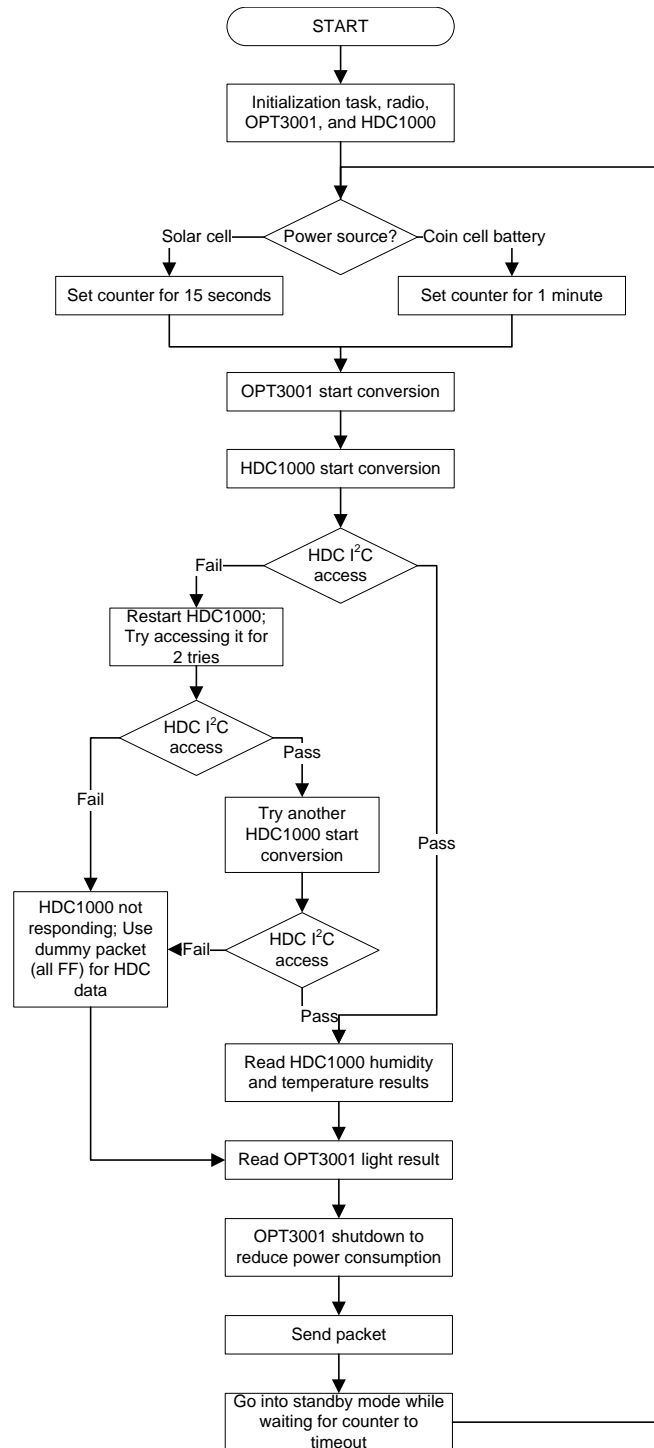


図 10. Firmware Flowchart

The flowchart shown in 図 10 consists of the CC1310 operating in continual transmission mode. It starts with initializing the wireless MCU peripherals and I/O ports.

In the infinite loop of measurement, the CC1310 first determines the power source to determine the rate for sensor measurement and wireless communication. If the power source is the solar cell, a shorter interval time of 15 seconds will be used. If the power source is the coin cell, a longer interval time of 60 seconds will be used to conserve battery life. Then, the CC1310 triggers the OPT3001 and HDC1000 to start the conversion. Because the HDC1000 has a higher operating voltage compared to the OPT3001 and CC1310, a check is added to make sure that the HDC1000 is still functioning at the lower operating voltage. If the voltage is too low for the HDC1000 is function properly, the HDC1000 conversion is aborted and dummy HDC data will be used.

As the OPT3001 and HDC1000 are converting, the CC1310 goes into standby mode. The CC1310 will wake up and read the results when either the HDC1000 or OPT3001 data ready line becomes active. After the CC1310 has acquired the temperature, humidity, and light data, a packet with the data will be transmitted. No additional configuration is needed for the HDC1000 and OPT3001 because the devices will automatically go into low power mode after a conversion. The CC1310 will enter standby mode again and wait for the interval counter to timeout before the next cycle of measurement.

5 Getting Started Hardware

5.1 Hardware Overview

Figure 11 shows the hardware for the Energy Harvesting Ambient Light and Environment Sensor Node for Sub-1GHz Networks TI Design. The PCB is in a 2.0x3.0-in rectangular form factor and comes with 0.5-in nylon standoffs to ensure ease of use while performing lab measurements.

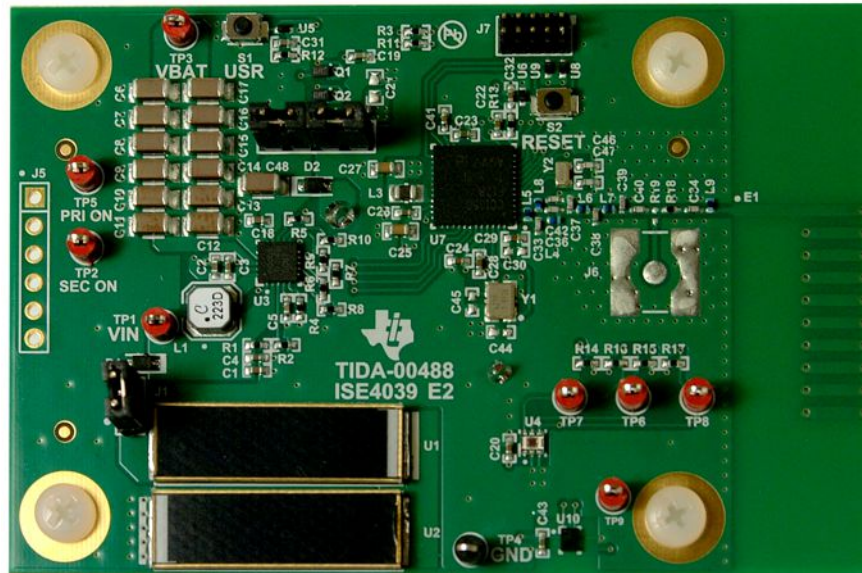


Figure 11. Energy Harvesting Ambient Light and Environment Sensor Node for Sub-1GHz Networks Reference Design Hardware

For both the solar cells to charge the capacitor reservoir, short jumper J1 with a jumper shunt. Short pins 1 and 2 of J4 with a jumper shunt to power the system from the battery when the solar energy is not high enough to charge the capacitor reservoir or maintain continuous system operation. Also short pins 3 and 4 on J4 with a separate jumper shunt to connect the output of the bq25505 to the sensor nodes and the CC1310.

5.2 Loading Firmware

The firmware used on this TI Design was developed using TI's [Code Composer Studio](#) software (version 6.1.0).

The IAR Embedded Workbench for ARM () also supports the CC13xx line of SimpleLink products.

To program or debug the TI Design hardware, no jumper shunts are required because the bq25505 does not need to be programmed internally; it only requires external voltage dividers for voltage-level settings for its internal power management.

Powering the board from 3.0 V is also necessary and can be supplied at pin 3 on J4.

The TI Design hardware is programmed by connecting the 10-pin mini ribbon cable from J7 to the SmartRF06 Evaluation Board (10-pin ARM Cortex Debug Connector, P418). See [Figure 12](#) for a photo of the correct setup for connecting the TI Designs hardware to the SmartRF06 evaluation board.

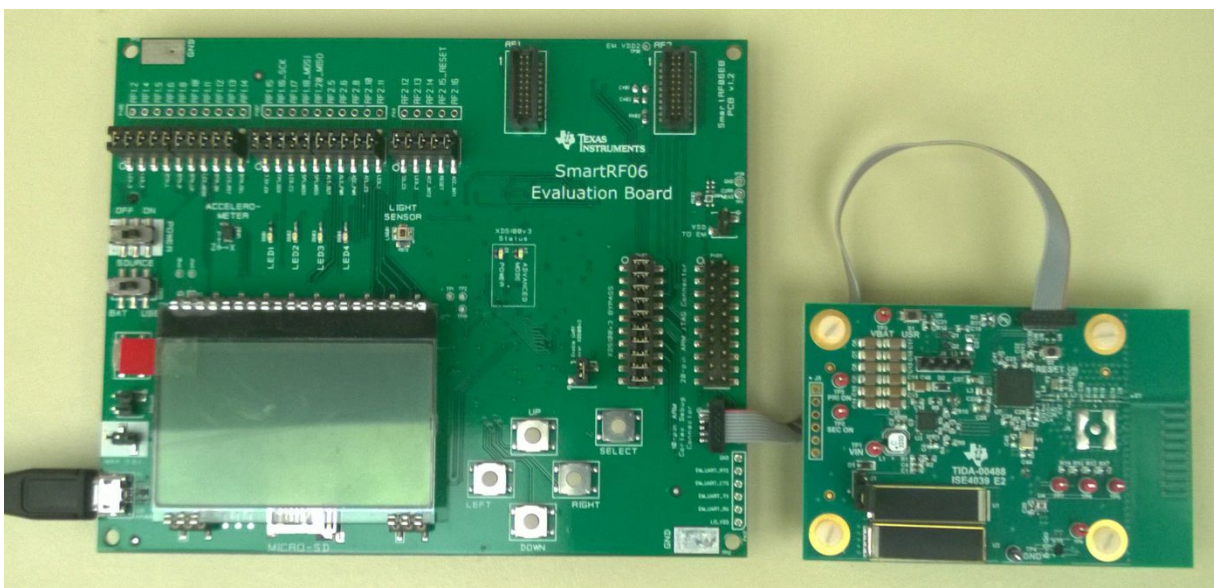


Figure 12. Connection of SmartRF06 Evaluation Board and TI Designs Hardware for Programming and Debugging

There are two different programs that were used for operating this TI Design; one is for the continual transmission ambient sensing option while the other is for the interrupt-based ambient sensing option.

5.3 Receiving Data Packets

This TI Design is designed to read light, relative humidity, and temperature data from the OPT3001 and HDC1000, respectively. The CC1310 is then to broadcast that data as a non-connectable data packet. The packets consist of two bytes for the TI design identifier, two bytes of relative humidity data, two bytes of temperature data, and two bytes of light data.

To verify the proper operation of the radio transmission, two methods to view the transmitted packet are described in the next two sections.

5.3.1 Building Automation Sub-1GHz Sniffer Application

The first method is a sniffer application running on the SmartRF06 EVM with the CC13xxEM radio. The sniffer application will process the received packet and display the calculated data on the LCD screen.

The LCD screen will show the six most current received data. If more data is needed for testing or characterization purposes, 5.3.2 describes how to get more data samples for post analysis.



図 13. Sniffer Application Running on the SmartRF06 EVM With the CC13xxEM Radio

For more information about the sniffer GUI, download and install the Building Automation Sub-1GHz Sniffer software package available in 8.8 of the TI Design tools page.

5.3.2 CC1111 USB Dongle and SmartRF Protocol Packet

The second method uses the [CC1111 USB Dongle](#). The CC1111 USB EVM Kit 868/915 MHz "sniffs" packets using the [SmartRF™ Protocol Packet Sniffer](#) software. The data will be displayed as raw data stream. This data stream can be post processed and used for testing and characterization. After installing the packet sniffer software (v2.18.1 at the time of writing), the procedure is as follows to detect the data transmissions:

1. Plug the CC1111 USB dongle into an unused USB port on the computer with the packet sniffer software installed.
2. Open the packet sniffer software; choose Generic as the protocol and click the Start button (see [Figure 14](#)).

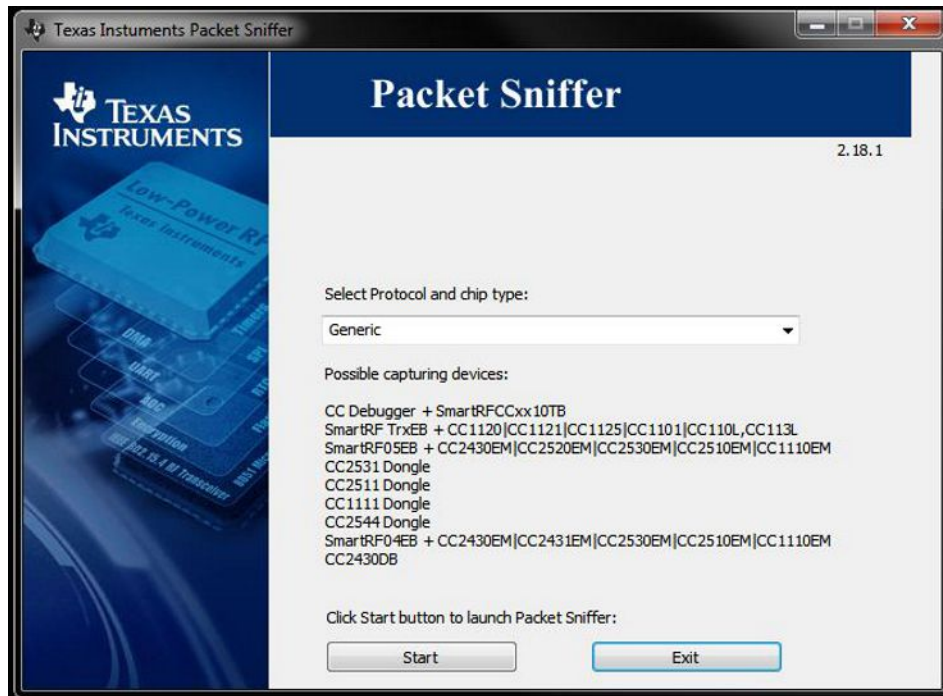


Figure 14. Packet Sniffer Start Screen

- Configure the CC1111 correctly to see the packets. Select the Radio Configuration tab. Under the Register settings sub tab, click on the "Browse..." button. Open the TIDA-00488_CC1111.prs file. Highlight and double-click on "TIDA-00488_CC1111" to apply the register settings shown in [Figure 15](#).

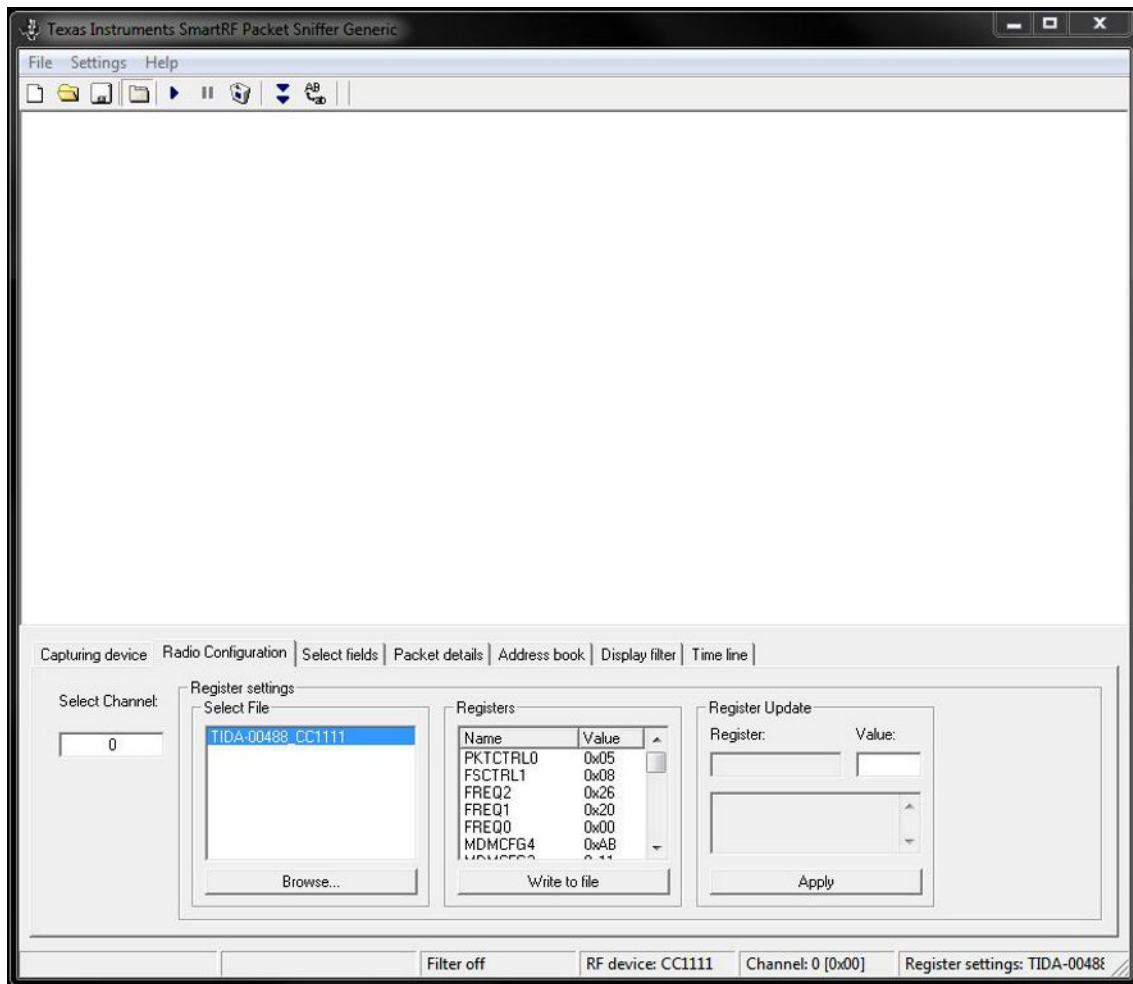


Figure 15. Radio Configuration and Monitor Screen

注: If long data acquisition periods are expected, increase the Cache Buffer size in the packet sniffer software to prevent possible crashes. Take this action by opening the Settings menu and clicking "Cache buffer size...".

4. Press the Play button on the top toolbar to initiate the packet capture process.
5. The packet sniffer software is likely to detect many other packets. Apply a display filter to view only the valid data packets.

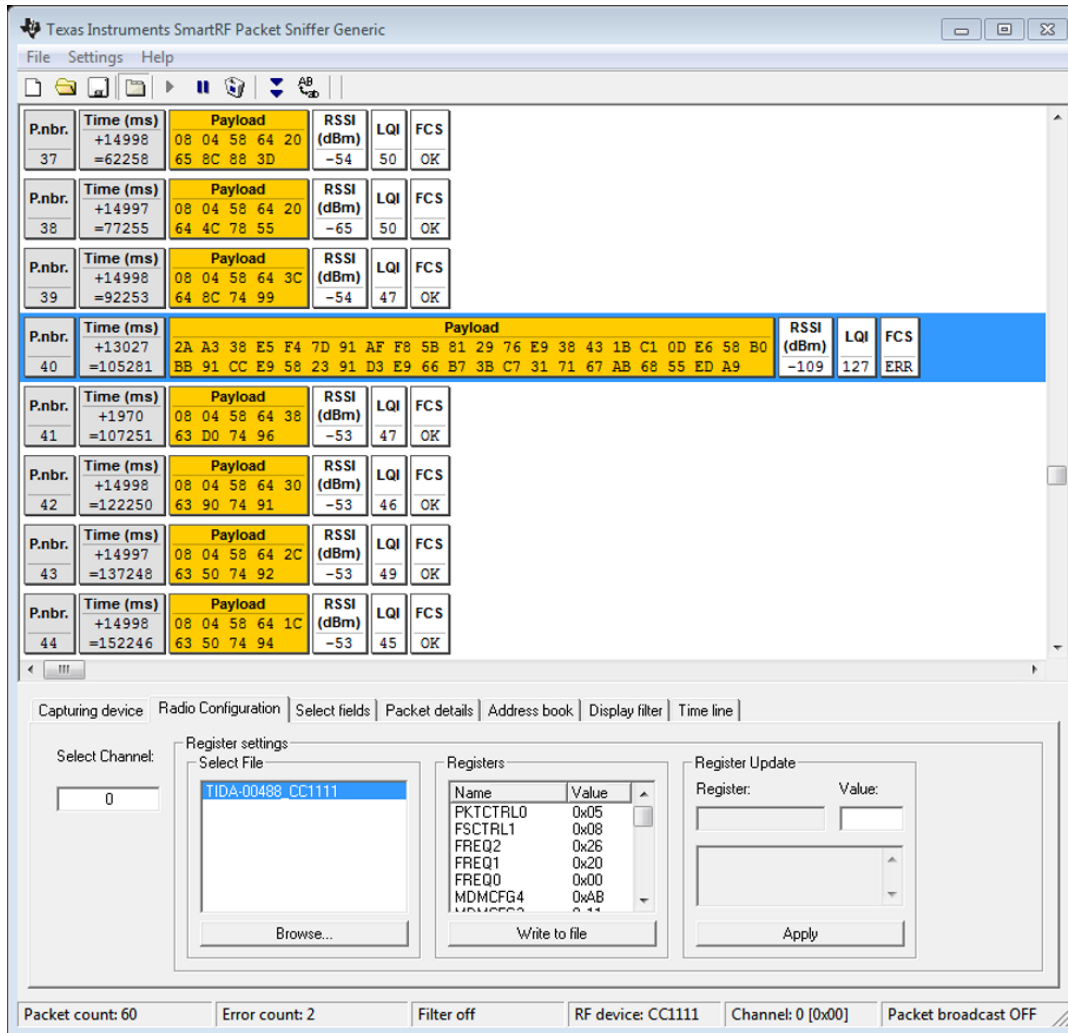


図 16. Unfiltered Radio Data

- The appropriate filter checks for only valid packets. In the Field Name field, select "FCS" from the dropdown options. Click the button labeled "First." Modify the filter condition to only show "OK" packets by typing "FCS=OK" in the Filter condition field, click the "Add" button, and then click the "Apply" filter button. The screen capture in [Figure 17](#) shows an example filtered view.

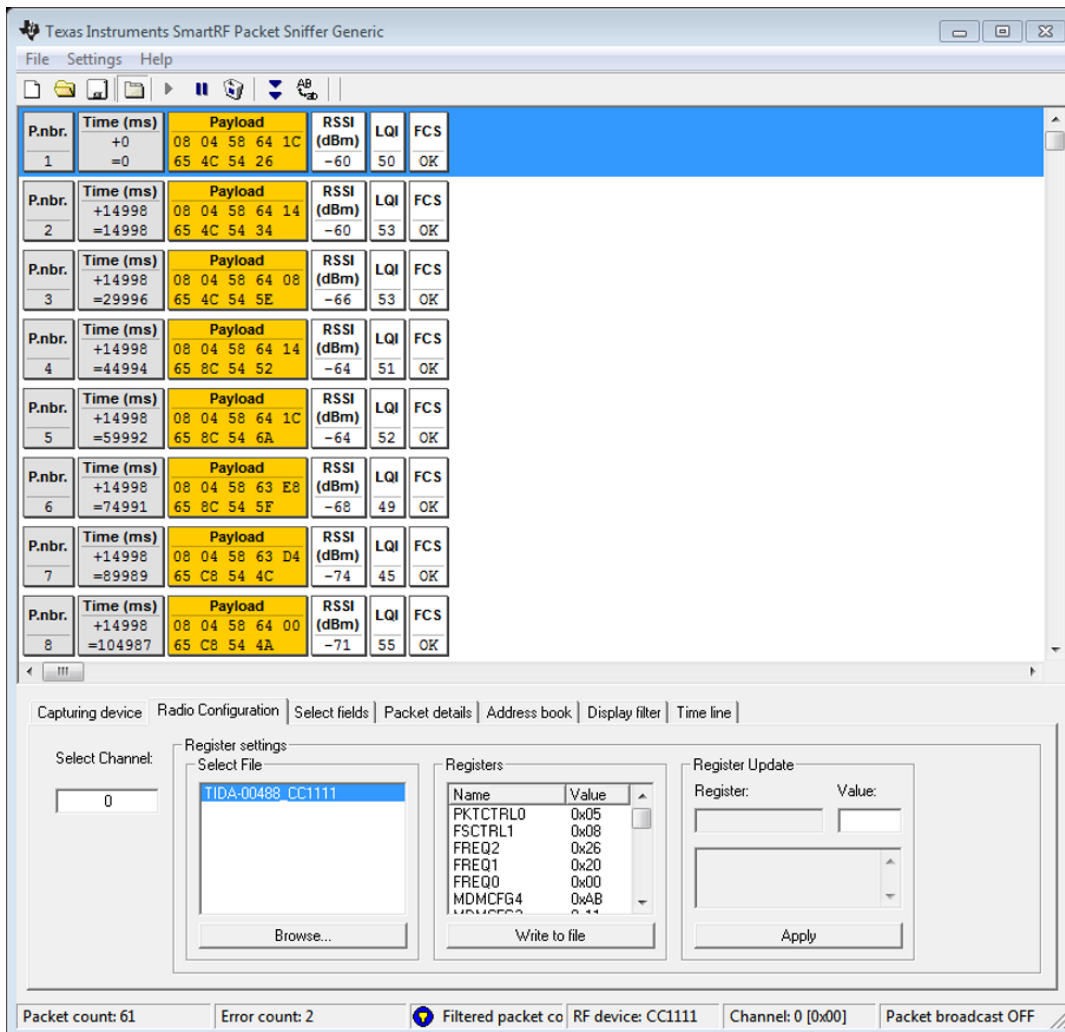


Figure 17. Filtered Radio Data

- To export the captured filtered packets, click the "Save the current session" button on the toolbar (appears as a floppy disk), or pause the packet capture and click File → Save data... from the file context menu; either of these choices prompts to save the displayed data as a packet sniffer data (.psd) file.
- Use HexEdit software (<http://www.hexedit.com/>) to convert the .psd file to readable hex values. A different hex editor may perform this function as well; however, the authors of this document have not verified any other options.
- Open the .psd file in the HexEdit software. Click on Tools → Options. In the HexEdit Options window, click on Document → Display and change the Columns value to "2066". Click Edit → Select All and Edit → Copy As Hex Text. Open a text editor program (for example, Notepad), paste the hex text, and save the text file. This text file can then be imported into Microsoft® Excel® spreadsheet software for further analysis. For more information on the sniffer data packet format, click Help → User Manual on the packet sniffer software.

6 Test Data

As described in 4.2, the TIDA-00488 firmware provides data packets continuously. The system is powered by the solar cells U1 and U2 or by the CR2032 battery. When the light level is sufficient, the bq25505 stores energy harvested by the solar cells on a bank of capacitors and controls whether the system is powered by the stored energy or by the primary cell.

The continual transmission ambient sensing application for the Energy Harvesting Ambient Light and Environment Sensor Node for Sub-1GHz Networks TI Design is intended to rely primarily on ambient light for system power, using a CR2032 coin cell as a backup power source only. This application of the TI Design has been characterized for optimized power management and power consumption.

The TIDA-00488 is optimized for use near a window that allows direct sunlight into a building. To simulate the light levels experienced near a window, the day time light level was measured in a slightly dirty, south facing window with an ultra-violet (UV) coating film installed. The dirt and UV film attenuate the solar rays significantly. Measurements were made under several conditions. In mid-morning, before the sun was shining directly into the window, the light level was about 1,000 lux. Mid-day light levels were closer to 5,000 lux when the sky was clear and about 3,200 lux when a cloud was passing over the sun on a partly cloudy day. Indoor ambient light levels away from the window varied from 250 to 450 lux depending upon the location.

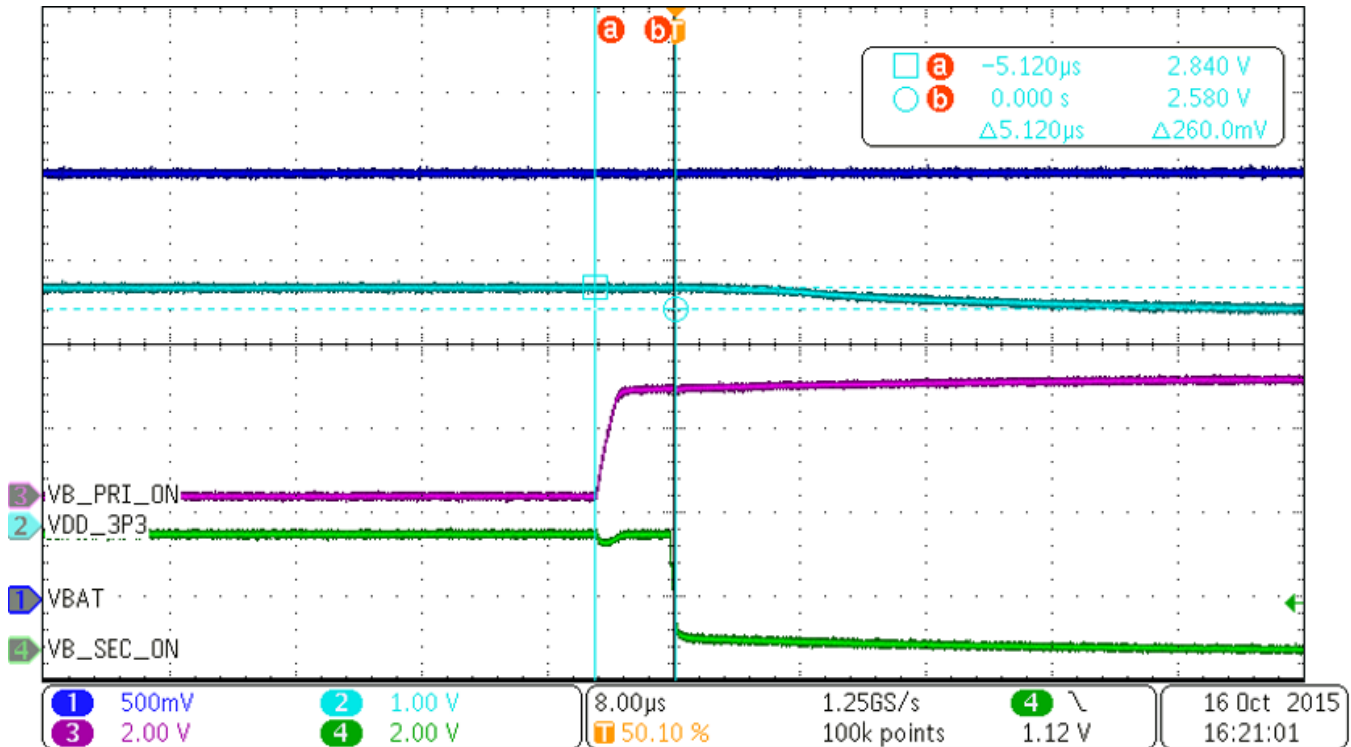
The oscilloscope used in the following tests is a Tektronix MDO3024 Mixed Domain oscilloscope with a Tektronix TCP0030A current probe for current readings. Current below 1 mA is measured with a Keysight/Agilent 34410A 6½ Digital Multimeter (DMM).



図 18. Light Meter Measuring Light Level in a Sunny Window

6.1 Transition Voltage

The bq25505 is programmed to power the system from the CR2032 primary cell until the capacitor reservoir (C6 through C17) voltage reaches 2.5 V. The system is then powered from the capacitor reservoir.  19 shows the power transition.



 19. Power Transition From Primary Cell to the Capacitor Reservoir Charged by the Solar Cells

In the figures in this section, there are four oscilloscope traces:

- The dark blue trace is the voltage of the capacitor reservoir, VBAT, measured at test point TP3
- The purple trace is the signal VB_PRI_ON
- The green trace is signal VB_SEC_ON
- The light blue trace is the voltage VDD_3p3 that powers the CC1310 and the two sensors

In  19, VBAT is 2.5 V. The cursors show that VDD_3p3 starts at 2.84 V and drops to 2.58 V after the transition to solar power. During the test, the battery voltage was 3.086 V when measured with a DMM. The drop to 2.84 V is caused by reverse protection diode D2.

Signal VB_PRI_ON controls Q2. When VB_PRI_ON is low, the system is powered by the primary cell. Signal VB_SEC_ON controls Q1. When VB_SEC_ON is low, the system is powered by the solar cell and capacitor reservoir. In  19, there is a 5.12- μ s period in which the power to the system is not connected to either the primary cell or the capacitor reservoir. This is a very short duration for this system, so there is no significant voltage drop to the system during the transition.

When the system is being powered by the capacitor reservoir, the system power is switched to the primary cell when the reservoir voltage drops to 1.9 V. [Figure 20](#) shows the power transition from the solar cell and capacitor reservoir to the primary cell.

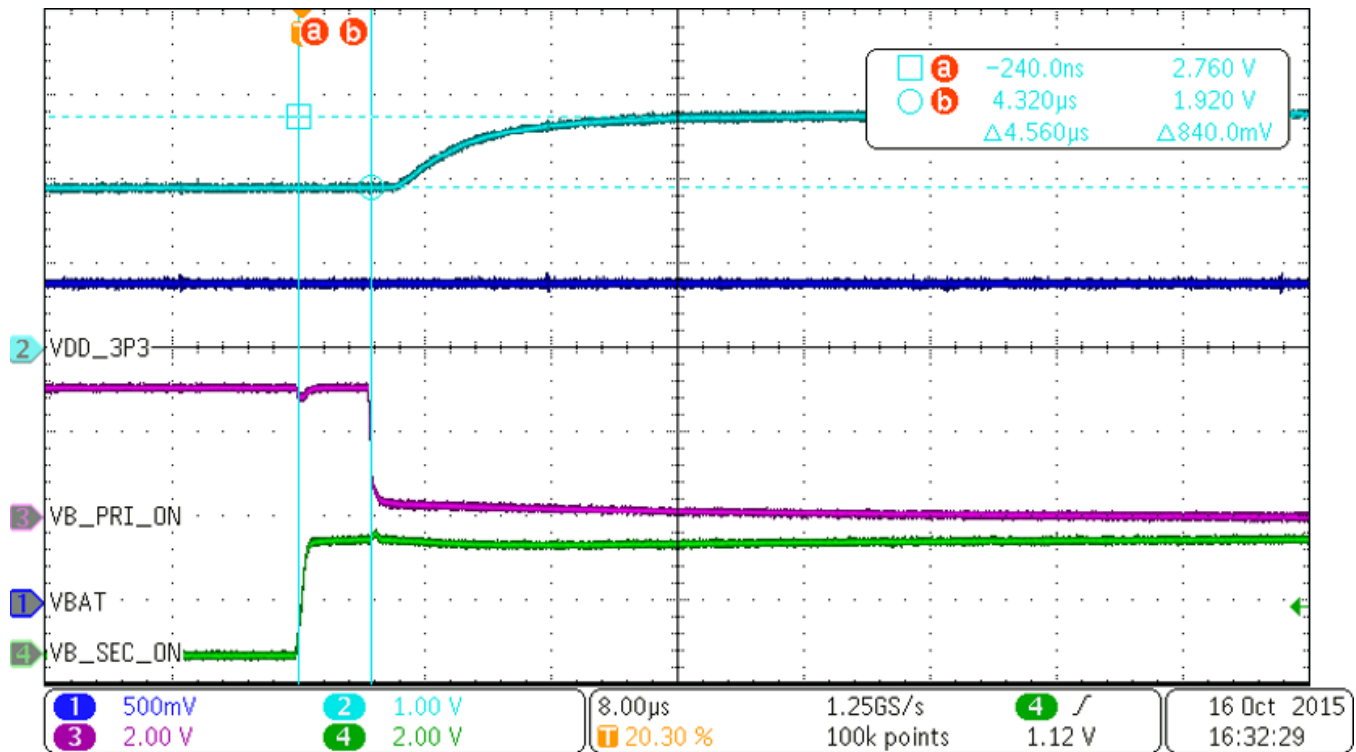


Figure 20. Power Transition From Primary Cell to the Capacitor Reservoir Charged by the Solar Cells

The trace colors in [Figure 20](#) represent the same signals as in [Figure 19](#). The capacitor reservoir voltage here is 1.92 V. The battery voltage minus the D2 voltage is 2.76 V. There is a 4.56- μ s period in which the power to the system is not connected to either the primary cell or the capacitor reservoir.

6.2 Solar Cell Capacitor Reservoir Charge Time

The amount of energy provided by the solar cells varies depending upon the amount of light incident on the cells. A higher lux level charges the capacitor reservoir faster. The results in this section use light levels of 1,000 lux, 2,000 lux, and 4,000 lux. Light levels were measured with an Extech Instruments model 407026 light meter. The primary light source during the tests was a Fostec Ace I adjustable light attached to a microscope that could be raised and lowered to help adjust the light level. Some ambient light also made up part of the incident light. The light level was measured near the center of the light spot provided by the microscope light. The light meter sensor was then moved away and the TIDA-00488 system board under test was placed with the solar cells positioned in the same spot the light meter sensor had been in. The test setup is shown in [Figure 21](#).

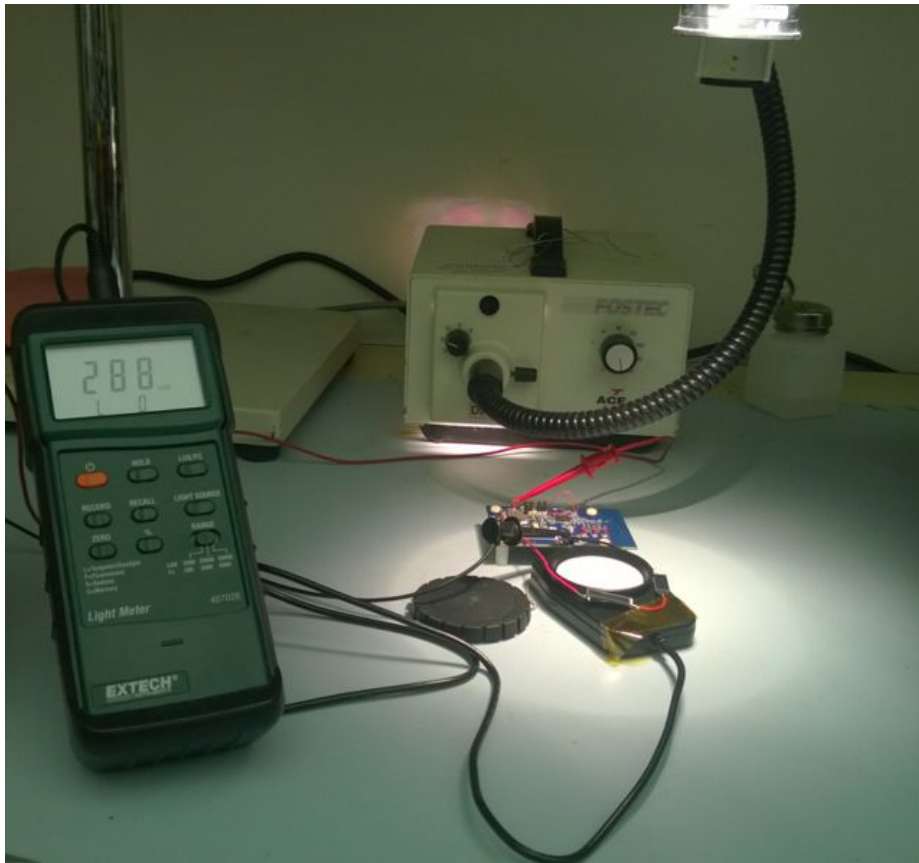


Figure 21. Light Measurement Setup With Microscope Light at 2880 Lux

The TIDA-00488 did not have the CR2032 battery installed during the charging tests. The voltage VBAT at test point TP3 was measured to determine the charging rate. The voltage at TP3 is measured with an oscilloscope to provide data over the long period of time the capacitor reservoir takes to discharge. A DMM is also connected between TP3 and ground to give instantaneous feedback of the voltage. To begin the test, the jumper J1 is removed to disconnect the solar cells from the bq25505 boost charger. The capacitor reservoir is then discharged by connecting a resistor across one of the capacitors and allowing the measured voltage on the reservoir to drop to 30 mV or less. Once the oscilloscope is ready to trigger, jumper J1 is replaced and the capacitor reservoir is allowed to charge up.

Figure 22 shows the charge time for a 1,000-lux light level. There are several points of interest during the charging process. The capacitor reservoir is charged to 1.5 V at a very slow rate. This is the "cold start" period defined in the bq25505 datasheet. Above 1.5 V, the boost converter in the bq25505 starts and the charging rate increases greatly. Once the capacitor reservoir voltage reaches 2.5 V, the load is connected to the reservoir for power. When the load is connected, there is a large voltage drop as the bypass and filter capacitors in the main part of the system charge up. The capacitor reservoir charge rate slows down due to the intermittent load that is applied by the system during data collection and transmission. The CC1310 transmission cycle occurs every 15 seconds, which causes the jagged look of the oscilloscope trace as the voltage increases further. The capacitor reservoir continues charging until the voltage limit of 3.5 V is reached. Once 3.5 V is reached, the reservoir is recharged to 3.5 V after every transmission. Figure 22 shows that it takes about 435 seconds to charge to 1.5 V, 545 seconds to charge to 2.5 V, and about 700 seconds to charge to 3.5 V.

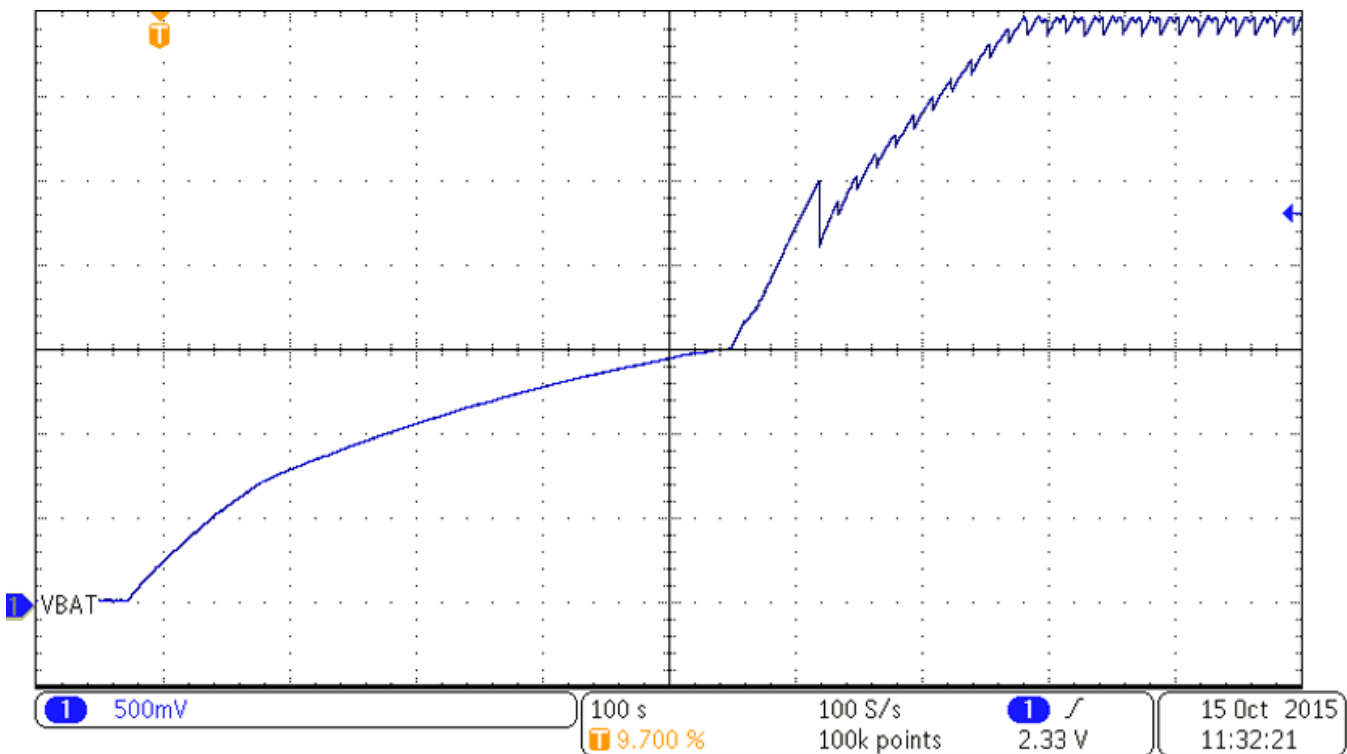


Figure 22. Capacitor Reservoir Charging Profile With 1,000 Lux Light Level

Charging curves for 2,000 lux and 4,000 lux are shown in [Fig. 23](#) and [Fig. 24](#).

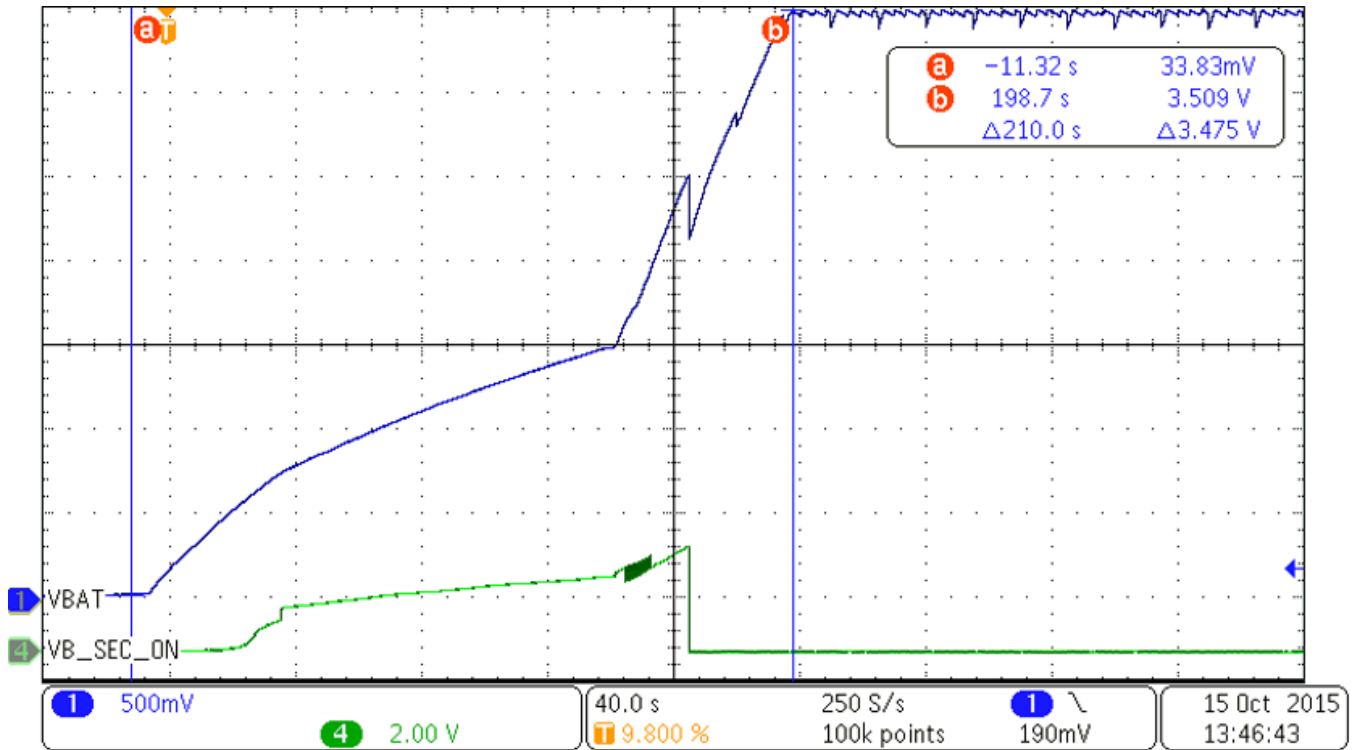


Fig. 23. Capacitor Reservoir Charging Profile With 2,000 Lux Light Level

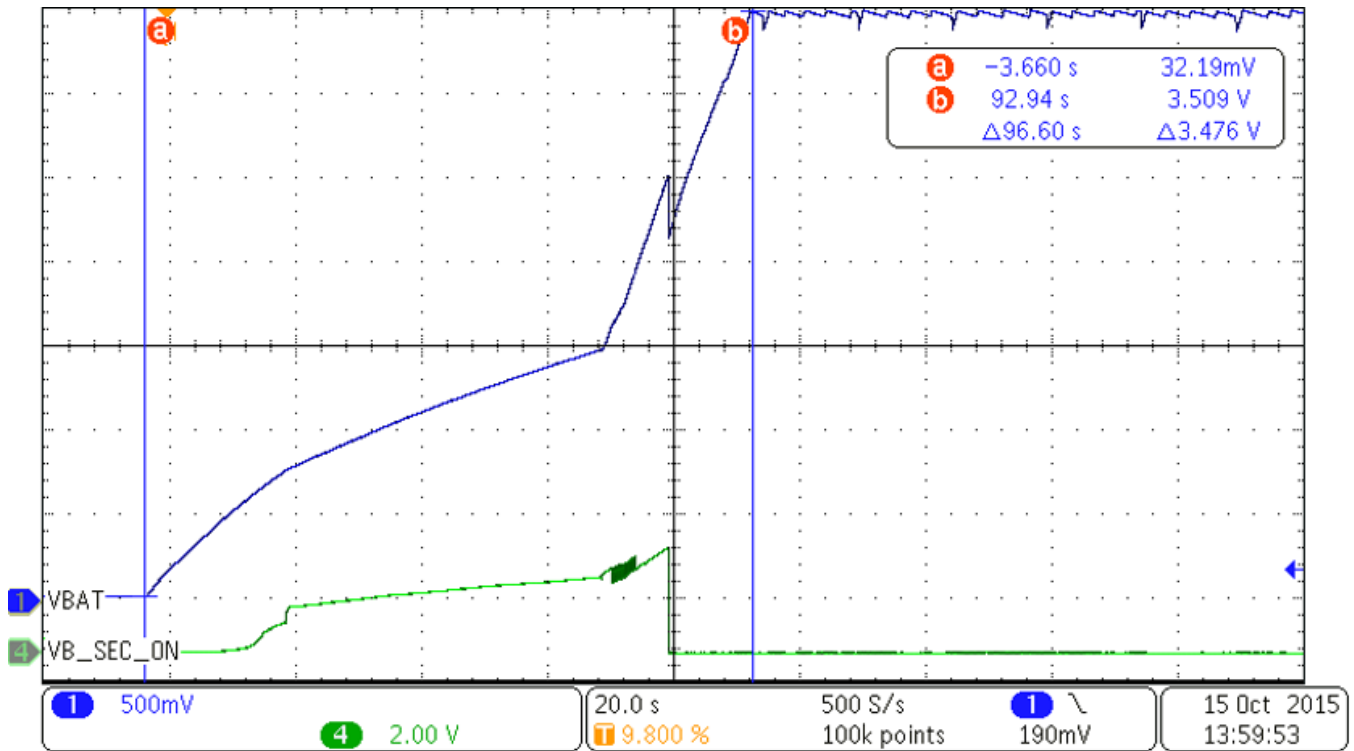


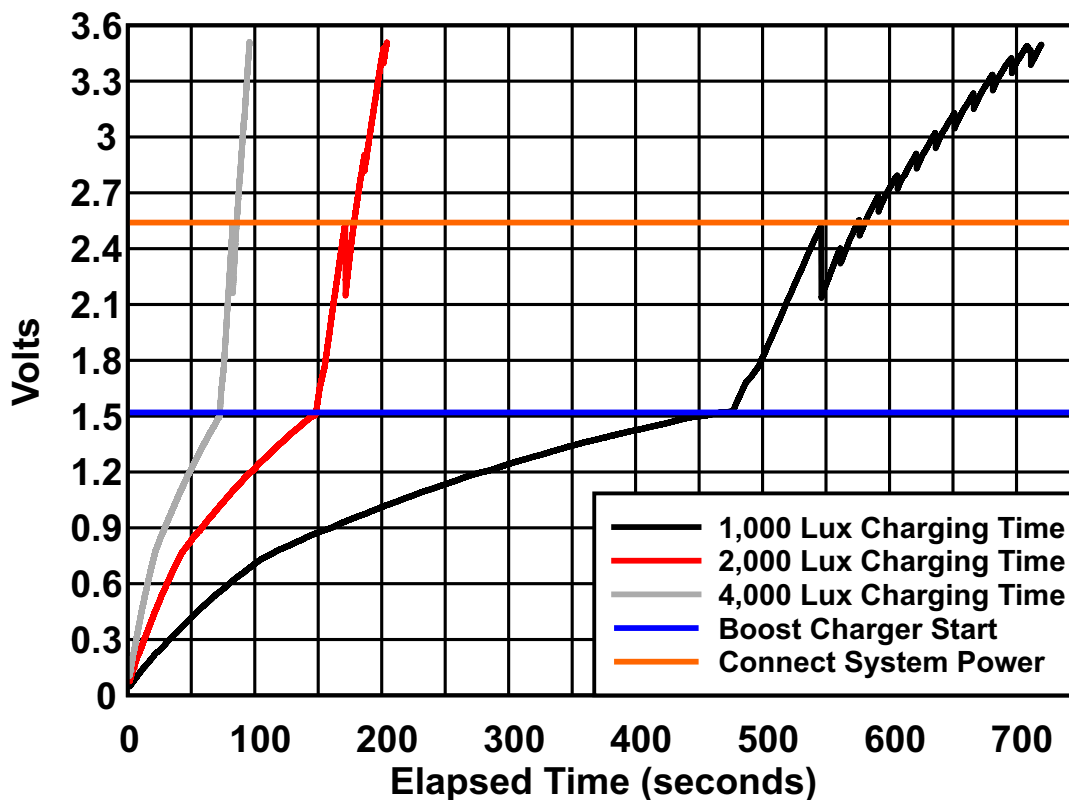
Fig. 24. Capacitor Reservoir Charging Profile With 4,000 Lux Light Level

The green trace in both  and  is the VB_SEC_ON signal described in 6.1. This was included to more clearly show when the system load was connected to the capacitor reservoir. The number of seconds per division is different in each view to help clearly show the detail of the VBAT trace as the charging time decreases. The charge times for all three lux levels are shown in .

表 2. Time to Charge the Capacitor Reservoir for Different Lux Levels

LUX LEVEL	TIME TO BOOST CHARGER START (s)	TIME TO CONNECT LOAD (s)	TIME TO 3.5 V MAXIMUM (s)
1000	435	545	700.0
2000	154	177	210.0
4000	73	83	96.6

 shows the three charge times plotted together.



 25. Voltage versus Time for the Capacitor Reservoir for Three Light Levels

The TIDA-00488 was able to harvest enough energy for operation with light levels as low as 750 lux. It took over 15 minutes to charge the capacitor reservoir to 2.5 V at 750 lux.

The capacitor reservoir charging curves presented here represent the worst case for the given light levels. In normal operation, a CR2032 battery is installed in the system to provide power when light levels are low. With the battery installed, the capacitor reservoir voltage does not drop significantly when the load is first switched to the capacitor reservoir because the bypass and filter capacitors will already be charged. The capacitor reservoir is unlikely to discharge to 30 mV when the system is in continuous use.

6.3 Current Profiles

The system current was measured in two ways. For the dynamic current measurements, an oscilloscope with a hall-effect current probe was used. This probe is not accurate for currents below 1 mA. For the very low current standby modes, a DMM with the capability to measure current to tenths of a microamp was used. System currents were measured with the system powered with a 3-V power supply unless otherwise noted.

6.3.1 Standby Current

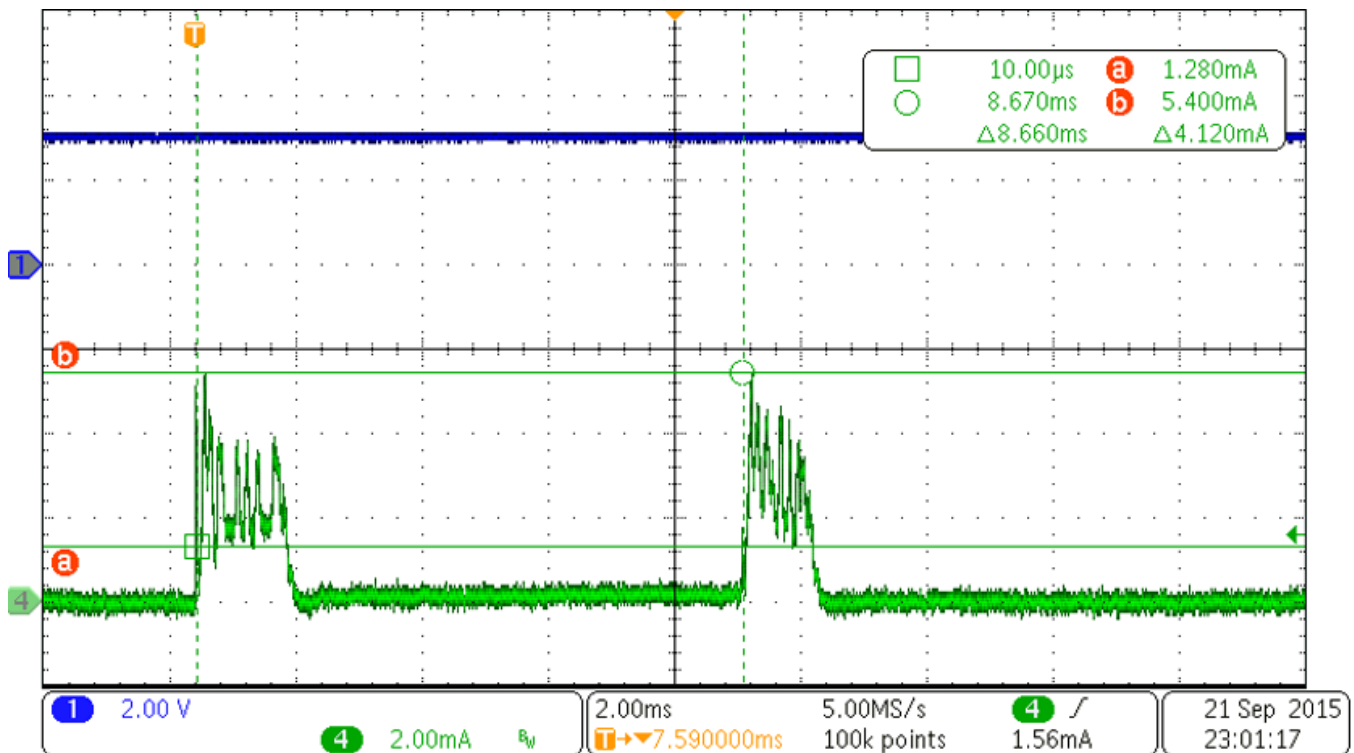
The standby current was measured using a DMM. During the system idle time, the average current was 1 μ A.

6.3.2 Current During Active Time

There are three periods of activity in continuous mode operation:

- In the first period, the CC1310 triggers the conversions in the light sensor and the temperature-humidity sensor.
- The second period is when the temperature-humidity sensor data is read.
- The third period is when the light sensor data is read and when the RF transmission occurs

☒ 26 shows the first two active periods.



☒ 26. Current Profile During Conversion Trigger and Temperature-Humidity Sensor Read

The initialization and read occur about 7 ms apart. The CC1310 enters the standby state between these times.

The second sensor read and data transmission occurs 100 ms after the first read (see [Figure 27](#)).

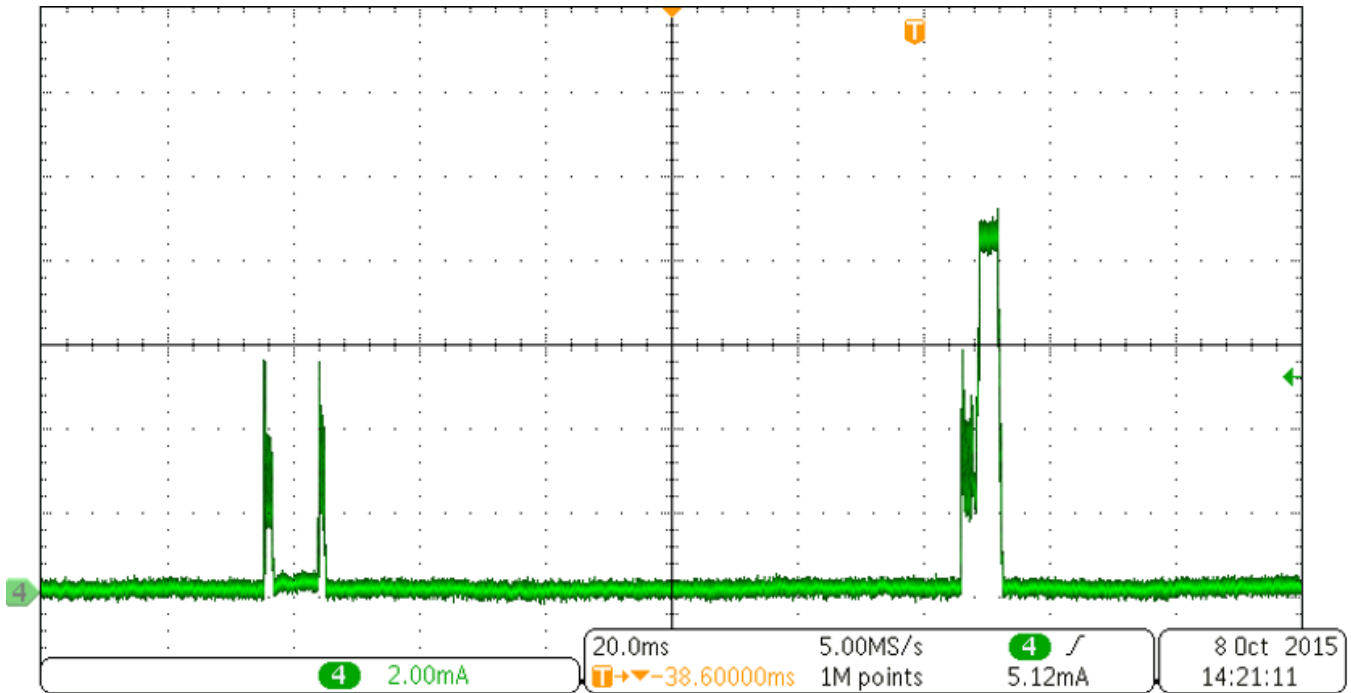


Figure 27. Current Profile of Sensor Data Conversions, Data Reads, and RF Transmission

A closer view of the light sensor data read and RF transmission current are shown in [Figure 28](#).

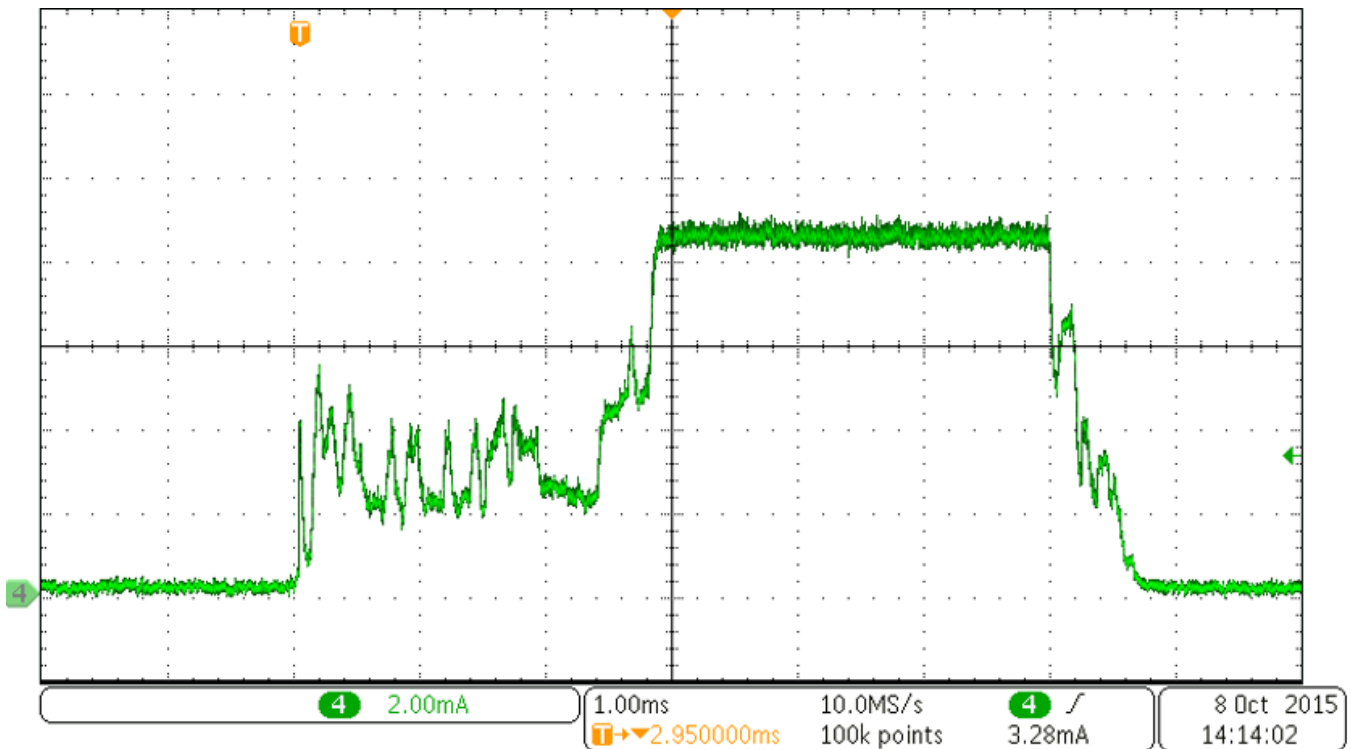


Figure 28. Light Sensor Data Read and RF Transmission

The total time the CC1310 is awake during the second sensor read and RF transmission period is 6.65 ms. The peak current of 8.7 mA occurs during data transmission.

Figure 29 shows the current during one complete 15-second transmit cycle.

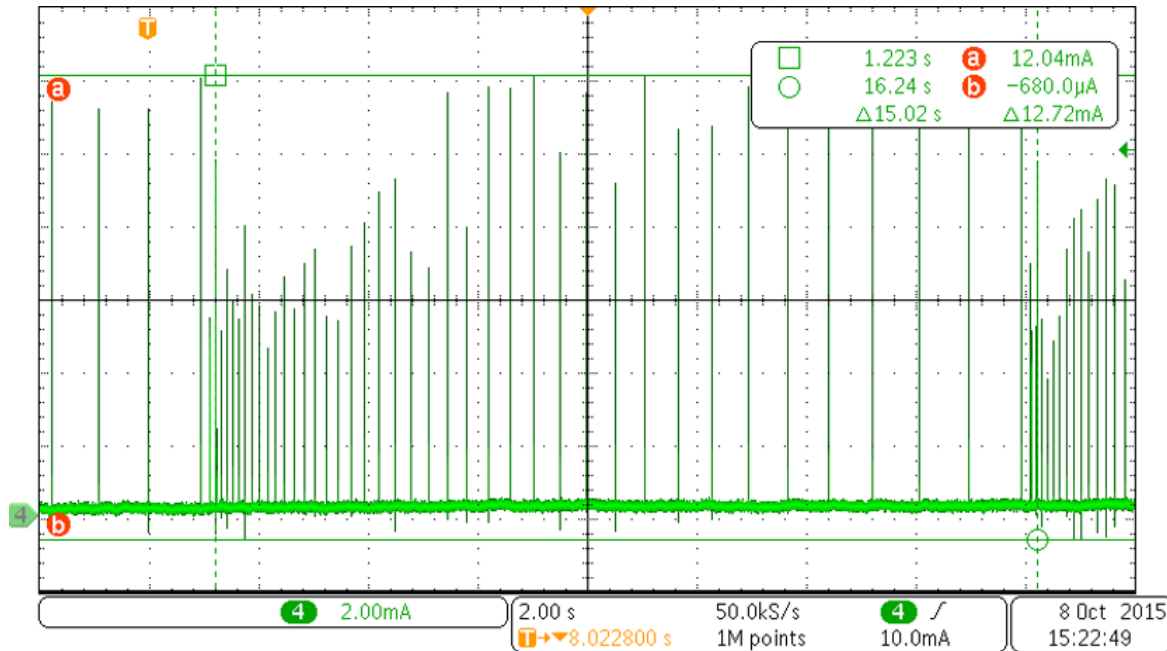


Figure 29. System Current Showing One Complete Transmit Cycle

注: The system was powered by a CR2032 battery during this trial.

During the 15-second cycle, there are several additional periods of current consumption. The current transients occur when the CC1310 DC-to-DC converter activates to maintain its regulated output voltage. These current transients are short. A typical current transient is shown in Figure 30. The current transients can be as high as 17.5 mA and the transients last about 190 μ s. Figure 29 shows there are about 39 of these transients during one 15-second transmit cycle.

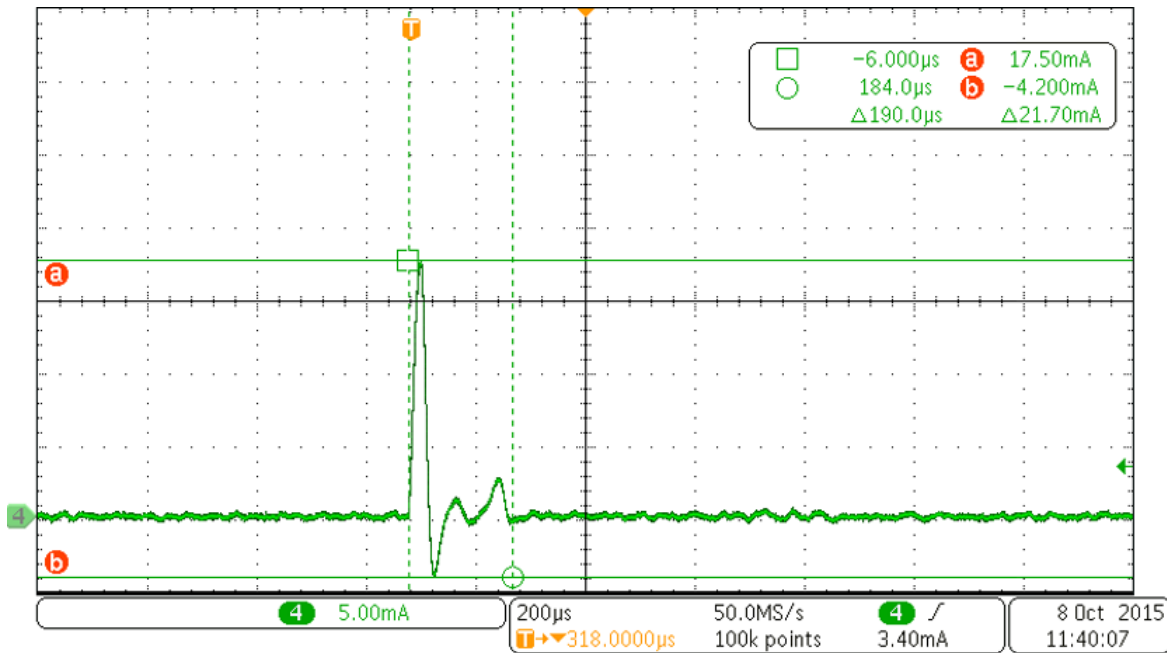


図 30. Current Transient During CC1310 Shutdown

The average current used during one cycle can be computed by finding the average current during the individual events shown in the previous figures. First, the average current during each event is calculated along with the total time for each event. The data for each of the graphs was saved so that accurate current averages and pulse widths could be determined. The amount of charge for each event was computed by multiplying the average current by the pulse width:

$$I_{AVG} \times t_{Event} = Q_{Event} \tag{7}$$

Where I is in amperes, t is in seconds, and Q is in coulombs. The current transient event occurs 39 times during a 15-second cycle, so 39 times that amount of charge is required during a cycle. For the portion of the cycle that is not part of one of these events, the CC1310 application processor is in shutdown mode. During that time, the current consumption of the system is only 1 μ A. 表 3 shows the results of the calculations.

表 3. Average Current and Total Charge During a 15-Second Transmission Cycle

EVENT	NUMBER OF EVENTS PER CYCLE	TIME (s)	AVERAGE CURRENT (mA)	AVERAGE CHARGE (C)	TOTAL CHARGE (C)	TOTAL TIME (s)
Sensor initialization	1	0.001460	2.360	3.45E-06	3.45E-06	0.001460
Sensor read 1	1	0.001254	2.490	3.12E-06	3.12E-06	0.001254
Sensor read 2 and transmission	1	0.006650	5.680	3.78E-05	3.78E-05	0.006650
Current transient	39	0.000182	2.120	3.86E-07	1.51E-05	0.007098
Standby time		14.987950	0.001	1.50E-05	1.50E-05	14.981040
Grand totals			4.96E-03		7.44E-05	14.997500

The total cycle time was found to be 14.9975 seconds. Total charge is 74.4 μ C. Therefore, the average current is

$$I_{AVG} = \frac{Q_{Event}}{t_{Event}} \tag{8}$$

The average current during the cycle is 4.96 μ A.

Using this information, estimates can be made for shorter cycles. For an eight-second cycle between transmissions, there are still 30 current transients to maintain the CC1310 regulator voltage. For a five-second cycle, there are 23 current transients. Using the results in 表 3, the average current would be approximately 7.99 μA for an eight-second cycle and 11.64 μA for a five-second cycle. See 表 4 and 表 5 for the full results.

表 4. Average Current and Total Charge During an Eight-Second Transmission Cycle

EVENT	NUMBER OF EVENTS PER CYCLE	TIME (s)	AVERAGE CURRENT (mA)	AVERAGE CHARGE (C)	TOTAL CHARGE (C)	TOTAL TIME (s)
Sensor initialization	1	0.00146	2.36	3.45E-06	3.45E-06	0.00146
Sensor read 1	1	0.001254	2.49	3.12E-06	3.12E-06	0.001254
Sensor read 2 and transmission	1	0.00665	5.68	3.78E-05	3.78E-05	0.00665
Current transient	30	0.000182	2.12	3.86E-07	1.16E-05	0.00546
Standby time		7.985176	0.001	7.99E-06	7.99E-06	7.985176
Grand totals			7.99E-03		6.39E-05	8

表 5. Average Current and Total Charge During a Five-Second Transmission Cycle

EVENT	NUMBER OF EVENTS PER CYCLE	TIME (s)	AVERAGE CURRENT (mA)	AVERAGE CHARGE (C)	TOTAL CHARGE (C)	TOTAL TIME (s)
Sensor initialization	1	0.001460	2.360	3.45E-06	3.45E-06	0.001460
Sensor read 1	1	0.001254	2.490	3.12E-06	3.12E-06	0.001254
Sensor read 2 and transmission	1	0.006650	5.680	3.78E-05	3.78E-05	0.006650
Current transient	23	0.000182	2.120	3.86E-07	8.87E-06	0.004186
Standby time		4.986450	0.001	4.99E-06	4.99E-06	4.986450
Grand totals			1.16E-02		5.82E-05	5

In these three examples, the amount of charge used will be slightly higher. This is because the CC1310 application processor enters standby state during the period between sensor initialization and sensor read 1. The processor also enters standby during the period between sensor read 1 and sensor read 2 plus transmission.

6.4 Capacitor Reservoir Sizing

The capacitor reservoir has a nominal capacitance of 1200 μF . 6.2 shows that the charging rate of the capacitor reservoir for different light intensities. Lower light intensity results in a lower amount of charge generated by the solar cell. During the charging period, the amount of charge into the capacitor reservoir can be estimated using 式 9:

$$\Delta V \times F = \Delta Q_{\text{Reservoir}} \tag{9}$$

ΔV is the change in voltage on the capacitor reservoir, F is the reservoir capacitance, and ΔQ is the change in charge on the capacitor reservoir given the change in voltage. 図 31 shows a portion of the voltage rise during the charging of the capacitor reservoir when the light intensity is 1,000 lux.

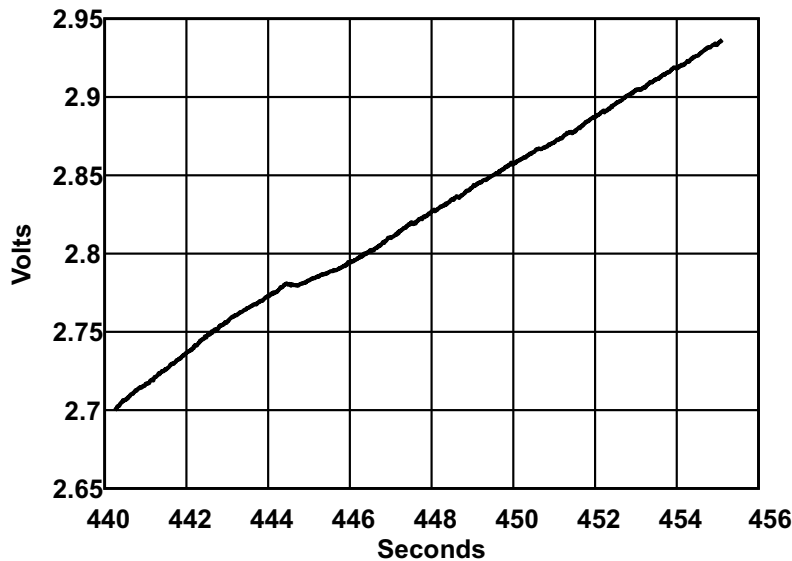


図 31. Voltage Rise Between Transmissions During Capacitor Reservoir Charging With 1000 Lux

The portion of the charging curve shown in 図 30 is only the portion that occurs between the times when the CC1310 is in shutdown mode. The capacitor reservoir can charge during this time. In this graph, $\Delta V = 0.237 \text{ V}$, so $\Delta Q = 0.237 \text{ V} \times 1,200 \mu\text{F} = 284 \mu\text{C}$. 6.3.2 shows that the system uses 74.4 μC during the 15-second transmission cycle. The difference between the amount of charge used by the system and the amount of charge added to the capacitor reservoir is $284 \mu\text{C} - 74.4 \mu\text{C} = 209.6 \mu\text{C}$, so the reservoir can continue charging.

The time period in 図 31 is 14.86 seconds. This is the time between the end of one RF transmission and the sensor initialization period. Once the system starts consuming energy from the capacitor reservoir, the voltage will drop. Since this time period is for a 15-second transmission interval, performance for shorter transmission intervals can be estimated by using the difference between the cycle times to adjust the charge time. Therefore, an eight-second RF transmission cycle would have a charge time of 7.86 seconds. The final voltage would then be about 2.82 V and the total accumulated charge would be 153 μC . The system could still run on the solar cell with an eight-second cycle, but the charging rate would be very slow after the system is connected to the reservoir. A five-second delay between transmissions would not provide enough time between transmissions to recharge the reservoir to the voltage it started from. The capacitor reservoir would deplete to 1.9 V quickly causing the system to run from the battery most of the time.

7 Notes About the Design

This design is useful where the solar cells are near a window and the average light level will be above 1,000 lux during a significant part of the system operating time. If energy harvesting operation is desired at lower light levels, more solar cells of the same type can be added. U1 and U2 are connected in series. To add more of the same type of solar cell, series pairs of cells could be added in parallel to the existing pair. The overvoltage and undervoltage levels for the bq25505 would not need to be changed in the design. Adding additional solar cell pairs in parallel increases the current available at lower light levels. A different type of solar panel could also be used in place of the existing panels at U1 and U2. In that case, the designer would need to adjust the bq25505 operating parameters to match the new solar cell.

8 Design Files

8.1 Schematics

To download the schematics, see the design files at [TIDA-00488](http://www.ti.com/energy-harvesting).

Energy Harvesting Power Management

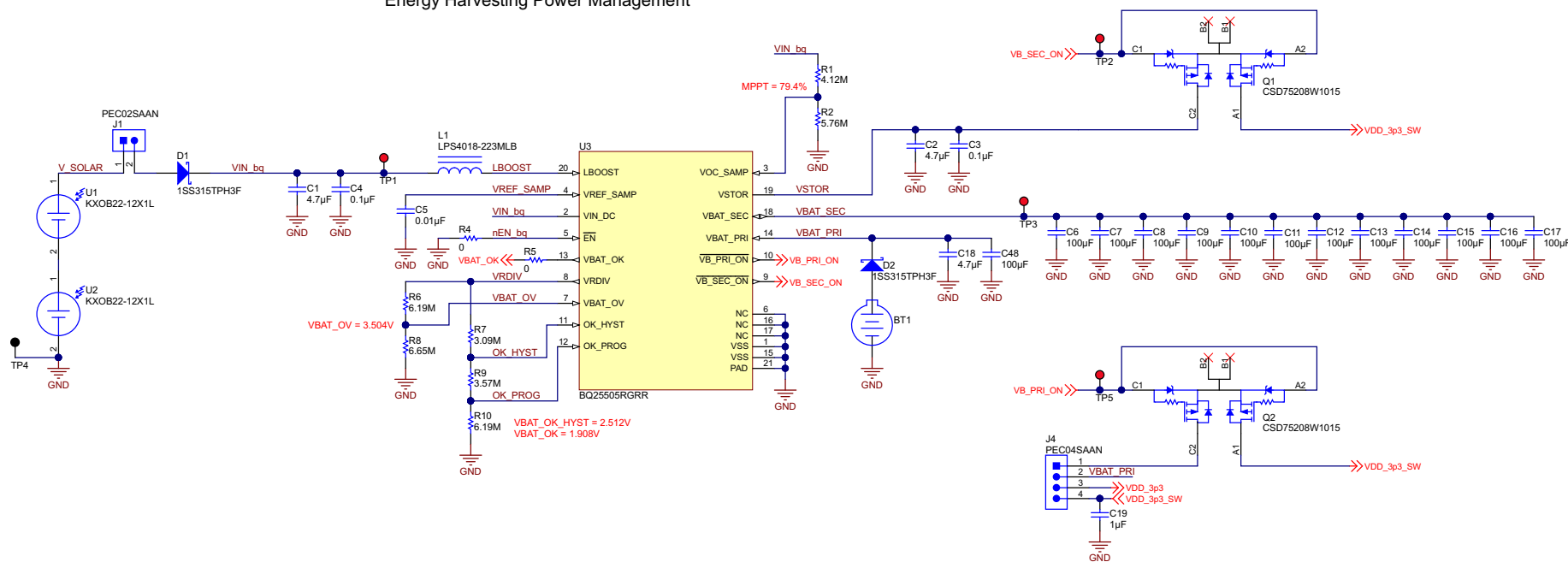


図 32. Energy Harvesting Schematic

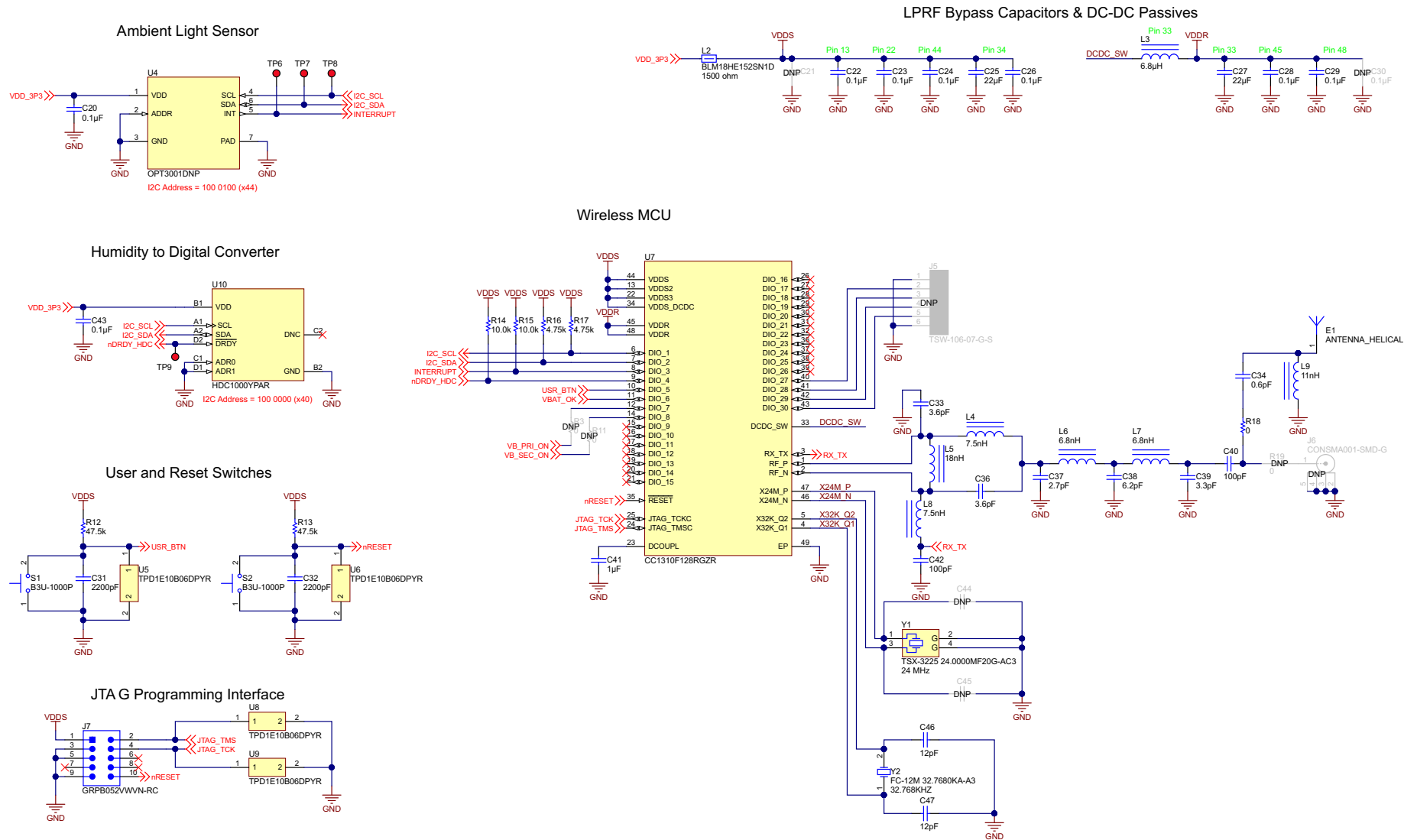


図 33. Bluetooth® and Light Sensing Schematic

8.2 **Bill of Materials**

To download the bill of materials (BOM), see the design files at [TIDA-00488](#).

8.3 **Layer Plots**

To download the layer plots, see the design files at [TIDA-00488](#).

8.4 **Altium Project**

To download the Altium project files, see the design files at [TIDA-00488](#).

8.5 **PCB Layout Recommendations**

To ensure high performance, the Energy Harvesting Ambient Light and Environment Sensor Node for Sub-1GHz Networks TI Design was laid out using a four-layer PCB. The second layer is a solid GND pour, and the third layer is used for power rail routing with GND fills in unused areas. The top and bottom layers are used for general signal routing and also have GND fills in unused areas.

For all of the TI products used in this TI Design, adhere to the layout guidelines detailed in the respective datasheets.

8.6 **Gerber Files**

To download the Gerber files, see the design files at [TIDA-00488](#).

8.7 **Assembly Drawings**

To download the assembly drawings, see the design files at [TIDA-00488](#).

8.8 **Software Files**

To download the software files, see the design files at [TIDA-00488](#).

9 References

1. Texas Instruments, *Ultra Low-Power Boost Charger With Battery Management and Autonomous Power Multiplexer for Primary Battery in Energy Harvester Applications*, bq25505 Datasheet ([SLUSBJ3](#))
2. Texas Instruments, *OPT3001 Ambient Light Sensor (ALS)*, OPT3001 Datasheet ([SBOS681](#))
3. Texas Instruments, *HDC1000 Low Power, High Accuracy Digital Humidity Sensor With Temperature Sensor*, HDC1000 Datasheet ([SNAS643](#))
4. Texas Instruments, *CC1310 Simplelink™ Ultra-Low Power Sub-1GHz Wireless MCU*, CC1310 Datasheet ([SWRS184](#))
5. Texas Instruments, *TPD1E10B06 Single-Channel ESD Protection Diode in 0402 Package*, TPD1E10B06 Datasheet ([SLLSEB1](#))
6. Texas Instruments, *Miniature Helical PCB Antenna for 868 MHz or 915/920 MHz*, DN038 Application Report ([SWRA416](#))

10 About the Authors

EVAN D. CORNELL is a systems architect at Texas Instruments where he is responsible for developing reference design solutions for the industrial segment. Evan brings to this role experience in system-level analog, mixed-signal, and power management design. Evan earned his master of electrical and computer engineering (M.Eng.) and bachelor of science (BS) in electrical engineering from the Rose-Hulman Institute of Technology in Terre Haute, IN. Evan is a member of the Institute of Electrical and Electronics Engineers (IEEE).

KELLY M. FERNANDEZ is an undergraduate student at the University of Maryland (UMD) where she is studying to receive her bachelor of science (BS) in electrical engineering. Her areas of interest include power electronics and energy harvesting. Kelly is also an undergraduate researcher in the Power Electronics, Energy Harvesting, and Renewable Energies Lab of the University of Maryland and is the President of her University's Institute of Electrical and Electronics Engineers (IEEE) student chapter.

MARK KNAPP is a systems architect at Texas Instruments where he is responsible for developing reference design solutions for the Building Automation segment. He has an extensive background in video camera systems and infrared imaging systems for Military, Automotive, and Industrial applications. Mark earned his BSEE at the University of Michigan-Dearborn and his MSEE at the University of Texas at Dallas.

CHRISTINA S. LAM is a systems architect at Texas Instruments where she is responsible for developing firmware for reference design solutions in the industrial segment. Christina has broad experience with applications processors, microcontrollers, and digital-signal processors with specialties in embedded firmware. Christina earned her bachelor of science (BS) in electrical and computer engineering from the University of Texas at Austin.

改訂履歴B

資料番号末尾の英字は改訂を表しています。その改訂履歴は英語版に準じています。

Revision A (December 2015) から Revision B に変更	Page
• to updated schematic 変更	48
• to updated schematic 変更	49

改訂履歴A

2015年12月発行のものから更新	Page
• プレビューページから 変更	1

TIの設計情報およびリソースに関する重要な注意事項

Texas Instruments Incorporated ("TI")の技術、アプリケーションその他設計に関する助言、サービスまたは情報は、TI製品を組み込んだアプリケーションを開発する設計者に役立つことを目的として提供するものです。これにはリファレンス設計や、評価モジュールに関する資料が含まれますが、これらに限られません。以下、これらを総称して「TIリソース」と呼びます。いかなる方法であっても、TIリソースのいずれかをダウンロード、アクセス、または使用した場合、お客様(個人、または会社を代表している場合にはお客様の会社)は、これらのリソースをここに記載された目的にのみ使用し、この注意事項の条項に従うことに合意したものとします。

TIによるTIリソースの提供は、TI製品に対する該当の発行済み保証事項または免責事項を拡張またはいかなる形でも変更するものではなく、これらのTIリソースを提供することによって、TIにはいかなる追加義務も責任も発生しないものとします。TIは、自社のTIリソースに訂正、拡張、改良、およびその他の変更を加える権利を留保します。

お客様は、自らのアプリケーションの設計において、ご自身が独自に分析、評価、判断を行う責任がお客様にあり、お客様のアプリケーション(および、お客様のアプリケーションに使用されるすべてのTI製品)の安全性、および該当するすべての規制、法、その他適用される要件への遵守を保証するすべての責任をお客様のみが負うことを理解し、合意するものとします。お客様は、自身のアプリケーションに関して、(1) 故障による危険な結果を予測し、(2) 障害とその結果を監視し、および、(3) 損害を引き起こす障害の可能性を減らし、適切な対策を行う目的で、安全策を開発し実装するために必要な、すべての技術を保持していることを表明するものとします。お客様は、TI製品を含むアプリケーションを使用または配布する前に、それらのアプリケーション、およびアプリケーションに使用されているTI製品の機能性を完全にテストすることに合意するものとします。TIは、特定のTIリソース用に発行されたドキュメントで明示的に記載されているもの以外のテストを実行していません。

お客様は、個別のTIリソースにつき、当該TIリソースに記載されているTI製品を含むアプリケーションの開発に関連する目的でのみ、使用、コピー、変更することが許可されています。明示的または黙示的を問わず、禁反言の法理その他どのような理由でも、他のTIの知的所有権に対するその他のライセンスは付与されません。また、TIまたは他のいかなる第三者のテクノロジーまたは知的所有権についても、いかなるライセンスも付与されるものではありません。付与されないものには、TI製品またはサービスが使用される組み合わせ、機械、プロセスに関連する特許権、著作権、回路配置利用権、その他の知的所有権が含まれますが、これらに限られません。第三者の製品やサービスに関する、またはそれらを参照する情報は、そのような製品またはサービスを利用するライセンスを構成するものではなく、それらに対する保証または推奨を意味するものでもありません。TIリソースを使用するため、第三者の特許または他の知的所有権に基づく第三者からのライセンス、あるいはTIの特許または他の知的所有権に基づくTIからのライセンスが必要な場合があります。

TIのリソースは、それに含まれるあらゆる欠陥も含めて、「現状のまま」提供されます。TIは、TIリソースまたはその仕様に関して、明示的か暗黙的にかかわらず、他のいかなる保証または表明も行いません。これには、正確性または完全性、権原、続発性の障害に関する保証、および商品性、特定目的への適合性、第三者の知的所有権の非侵害に対する黙示的保証が含まれますが、これらに限られません。

TIは、いかなる苦情に対しても、お客様への弁済または補償を行う義務はなく、行わないものとします。これには、任意の製品の組み合わせに関連する、またはそれらに基づく侵害の請求も含まれますが、これらに限られず、またその事実についてTIリソースまたは他の場所に記載されているか否かを問わないものとします。いかなる場合も、TIリソースまたはその使用に関連して、またはそれらにより発生した、実際の、直接的、特別、付随的、間接的、懲罰的、偶発的、または、結果的な損害について、そのような損害の可能性についてTIが知らされていたかどうかにかかわらず、TIは責任を負わないものとします。

お客様は、この注意事項の条件および条項に従わなかったために発生した、いかなる損害、コスト、損失、責任からも、TIおよびその代表者を完全に免責するものとします。

この注意事項はTIリソースに適用されます。特定の種類の資料、TI製品、およびサービスの使用および購入については、追加条項が適用されます。これには、半導体製品(<http://www.ti.com/sc/docs/stdterms.htm>)、評価モジュール、およびサンプル(<http://www.ti.com/sc/docs/sampterm.htm>)についてのTIの標準条項が含まれますが、これらに限られません。